Journal of Computational Mathematics
Vol.xx, No.x, 2023, 1–26.

http://www.global-sci.org/jcm
doi:10.4208/jcm.2303-m2022-0201

BÉZIER SPLINES INTERPOLATION ON STIEFEL AND GRASSMANN MANIFOLDS*

Ines Adouani[1)]
Department of Mathematics, University of Sousse, Tunisia
Email: ines.adouani.issatso@gmail.com
Chafik Samir
LIMOS-CNRS, University of Clermont Auvergne, France
Email: chafik.samir@uca.fr

Abstract

We propose a new method for smoothly interpolating a given set of data points on Grassmann and Stiefel manifolds using a generalization of the De Casteljau algorithm. To that end, we reduce interpolation problem to the classical Euclidean setting, allowing us to directly leverage the extensive toolbox of spline interpolation. The interpolated curve enjoy a number of nice properties: The solution exists and is optimal in many common situations. For applications, the structures with respect to chosen Riemannian metrics are detailed resulting in additional computational advantages.

Mathematics subject classification: 49K15, 65D10, 49K30.
Key words: Optimization, Bézier spline, Curve fitting, Grassmann manifolds, Stiefel manifolds, Canonical metrics.

1. Introduction

Data points on Riemannian manifolds are fundamental objects in many fields including, subspace filtering, machine learning, Signal-image-video processing and medical imaging [6, 7, 22]. To cite but few examples, tracking, face and action recognition and statistical shape analysis [1, 2, 35, 39, 42]. In many real-world applications, Stiefel manifold and Grassmann manifold are most commonly preferred as representation on Riemannian manifolds. A common limitation in many of these applications has been the geometric structure on underlying manifolds, e.g. Grassmann and Stiefel manifolds [1]. As increasingly real-world applications have to deal with non-vector data, a great number of algorithms for manifold embedding and manifold learning have been introduced. Recently, many efforts have been made to develop important geometric and statistical tools: Riemannian exponential map and its inverse, means, distributions, geodesic [6, 9, 25].

Motivated by the success of these approaches, we are interested in the problem of fitting smooth curves to a finite set of data points on a special class of Riemannian manifold $\mathcal{M}$: The Grassmann manifold of all p-dimensional subspace of $\mathbb{R}^n$ and the Stiefel manifold of p-orthonormal vectors in $\mathbb{R}^n$. More precisely, given a finite set of points $X_0, X_1, \cdots, X_N$ in $\mathcal{M}$ and a distinct and ordered instants of time $(0 = t_0 < t_1 < \cdots < t_N = 1)$, we seek a spline $\alpha : [0, 1] \to \mathcal{M}$ that best fits the given data $X_0, X_1, \cdots, X_N$ and is sufficiently smooth. More importantly, we focus on the search space of smooth regression splines where data points verify

* Received September 5, 2022 / Revised version received December 14, 2022 / Accepted March 27, 2023 / Published online November 22, 2023 /
1) Corresponding author

orthogonality constraints and t_i are distinct and ordered time instants. We show that this problem occurs in many real situations and leads to specific optimization methods, usually called optimization on Riemannian manifolds [1, 14]. In fact, one way to tackle the two conflicting goals of being sufficiently smooth while passing sufficiently close to the data points at the given t_i, is to express the spline α as the minimizer of the following functional:

$$\begin{aligned} E : \mathcal{W} &\to \mathbb{R}^+ \\ \alpha &\mapsto \frac{\lambda}{2}\int_{t_0}^{t_N} \left\langle \frac{D^2\alpha(t)}{Dt^2}, \frac{D^2\alpha(t)}{Dt^2} \right\rangle_{\mathcal{M}} dt + \frac{1}{2N}\sum_{i=0}^{N} d^2_{\mathcal{M}}\big(\alpha(t_i), X_i\big), \end{aligned} \tag{1.1}$$

where $\mathcal{W}$ denotes the underlying space of admissible C^2 splines in $\mathcal{M}$, $\langle .\,, . \rangle_{\mathcal{M}}$ and $d_{\mathcal{M}}$ denote the Riemannian metric and distance, respectively. We are thus facing an optimization problem in infinite dimension. It is well-known that when the Riemannian manifold $\mathcal{M}$ reduces to the Euclidean space $\mathbb{R}^n$, solutions of the optimization problem (1.1) under the interpolation constraint

$$\sum_{i=0}^{N} d^2_{\mathcal{M}}\big(\alpha(t_i), X_i\big) = 0$$

are cubic splines.

In this paper, we propose a geometric algorithm that generates a solution of problem (1.1), which is expressed as interpolating Bézier splines with a certain degree of smoothness. We adopt the Grassmann manifold as an example of symmetric spaces. Therefore, using the definition of geodesic curves and taking into account the rich and nice structure of these spaces, we present a novel approach to generate a C^2 Bézier spline that interpolates a given data set of points at specified knot times. As for the Stiefel manifold, in short, the task is that of regression on a homogeneous space [1] in the purpose to estimate/predict missing data from few available observations. By observations we mean any data points that can be obtained from temporal acquisitions. For example, medical images at different time instants are usually used to analyze the evolution of a disease. In this context and due to logistic and time constraints, it is very common to store few discrete moments only. Then at each time instant, we have a data point that is represented as an element of a manifold [25]. So there is a need to estimate missing data points on such manifold at non observed time instants. Several discrete-time models on smooth manifolds and Lie groups have been studied in the literature [34]. Here, we consider a continuous-time model only of class C^1 and will address the problem of regularized non-linear regression from finite observations [12]. In the main and in both cases, we start from the energy minimization formulation of linear least-squares in the Euclidean space $\mathbb{R}^n$ and generalize this concept to these manifolds. The proposed method is geometrically simple, extensible and easy to implement. In fact, we illustrate the relevance of the proposed method with various experiments.

In a general fitting problem, a vast number of methods for fitting smooth curves to a given finite set of points on Riemannian manifolds have appeared recently. For instance, motivated by the work of Noakes *et al.* general Riemannian manifolds, the authors in [38] derive a fourth-order differential equation associated to this variational problem involving the covariant derivative and the curvature tensor and prove that the optimal curves are approximating cubic splines. On the other hand, Samir *et al.* [36] choose to solve the optimization problem (1.1) by means of a steepest-descent algorithm on an adequate set of curves where the steepest-descent direction for the energy function E is defined with respect to the first-order and second-order Palais

metric. Jupp and Kent proposed a regression method on the sphere based on the technique of unrolling [21]. This approach was recently generalized by Kim *et al.* [22] to shape space. Niethammer *et al.* [28] solved the optimization problem (1.1) on the manifold of diffeomorphisms using an adjoint method. Other alternative approaches, but without a variational interpretation have been developed. These approaches includes subdivision schemes [13, 27, 41], Lie-algebraic methods [37], intrinsic polynomial regression [17], extrinsic local regression [26], global and local Fréchet regression [31]. Neither of these methods can be used for constructing C^2 interpolating splines on Riemannian manifolds which is the main motivation of this paper. In this direction, various works have been introduced to construct an interpolating Bézier spline on Riemannian manifolds of class C^1. We mention [16] (and references therein) for an account of important theoretical contributions in this area. Unfortunately, the problem of piecing generalized Bézier curves into a C^2 spline is much more complicated, except for some trivial cases such as compact Lie groups [10], spheres [32] and symmetric Riemannian manifolds [15, 33].

For the specific problem of interpolation on Grassmann and Stiefel manifolds $\mathcal{M}$, there exists a rich body of recent literature with an increasing interest. Indeed, Riemannian optimization on Stiefel and Grassmann manifolds is generally extremely hard to solve due to the geometric structure of $\mathcal{M}$ and to orthogonality constraints that represent these manifolds. Therefore, many efforts have been made to develop important geometric and statistical tools: Riemannian exponential map and its inverse, means, distributions, geodesic arcs, etc. [6]. For instance, Batzies *et al.* [3] have presented a simple closed form expression for the geodesic arc joining two points on Grassmann manifolds based only on the given data points. Hüper *et al.* [19] have proposed a scheme to compute the Karcher mean on Grassmann manifolds. However, only a little has been done in this direction for Stiefel manifolds. Edelman *et al.* [14] have derived an accurate expression of geodesics on Stiefel manifolds starting at a given point with a specified direction. Moreover, they propose numerical methods to compute exponential maps with both Euclidean and canonical metrics. Nevertheless, no explicit expressions for geodesic that joins two points on Stiefel manifolds are known.

To address this issue, in [29], the authors introduce the notion of quasi-geodesic, a curve with constant speed, constant covariant acceleration, and constant geodesic curvature that joins two points on the Stiefel manifold. In [34,43], they solved the problem by computing the Riemannian log map equipped with the canonical metric. We emphasize that methods for computing the Riemannian log map equipped with Euclidean metric have already been discussed in [5, 40]. By exploiting such explicit formulas, one can solve other important problems such as fitting and interpolation of data points on Grassmann and Stiefel manifolds. In this context, Hüper *et al.* [20] have proposed a method to generate interpolating curves on Grassmann manifolds which is based on the rolling technique. Batzies *et al.* [3] have deduced the necessary condition for the geodesic that gives the minimum value of the least-squares problem on Grassmann manifolds. Another method based on Jacobi field approach described by Rentmeesters [34] to approximate a given set of data points on the Grassmannian using gradient descent technique. We refer also to the recent paper [23] giving a new method to generate smooth interpolating curves on Stiefel manifolds. This method is achieved from a substitution of geodesic in the geometric De Casteljau algorithm on manifolds by a successive quasi-geodesic interpolation. Hong *et al.* [18] proposed an intrinsic geodesic regression model generalizing classical linear least-squares regression on Grassmannian.

The paper is organized as follows. In Section 2, we review the basic differential geometry of Grassmann and Stiefel manifolds that will be used to derive our main results. Section 3

introduces our approach to fit a given set of points on the Stiefel manifold. In Section 4, we address the fitting problem on the Grassmannian and we describe our method to construct a C^2 Bézier spline on this manifold. Section 5 shows numerical results and potential applications. We finish the paper with some concluding remarks in Section 6.

2. Preliminaries

In this section, we record some basic facts about Grassmann and Stiefel manifolds that will be essential in our terminology to build a consistent geometric algorithm to generate interpolating Bézier spline. In particular, we describe few computational tools (namely geodesics, the Riemannian Exp and Log maps) derived from a chosen Riemannian metric on these manifolds. For a more detailed exposition, we refer the reader to [1, 14].

2.1. A Riemannian structure of Stiefel manifolds

The compact Stiefel manifold $\mathcal{M} = St(n, p)$ is a matrix manifold of p-dimensional orthonormal frames in $\mathbb{R}^n$. As an embedded submanifold of $\mathbb{R}^{n\times p}$, $\mathcal{M}$ is defined by

$$\mathcal{M} = \{X \in \mathbb{R}^{n\times p} \mid X^T X = I_p\},$$

where I_p denotes the $p \times p$ identity matrix. When $p = 1$, we simply have the unit sphere S^{n-1}, while when $p = n$, we have the orthogonal Lie group $O(n)$ and when $p = n - 1$, we obtain the special orthogonal group $SO(n)$.

Remark 2.1. The Stiefel manifold can also be viewed as a quotient manifold of the orthogonal Lie group $O(n)$. In fact, two points Q_0 and Q_1 in the orthogonal Lie group $O(n)$ represent the same point in $\mathcal{M}$ if

$$Q_1 = Q_0 \begin{pmatrix} I_p & 0 \\ 0 & P \end{pmatrix}$$

for $P \in O(n - p)$. The linear left action of $O(n)$ in $\mathcal{M}$ is transitive (i.e. for every pair of elements X_1 and X_2, there is an element $Q \in O(n)$ such that $QX_1 = X_2$). Besides, the isotropy group at the identity frame

$$X = \begin{bmatrix} I_p \\ 0 \end{bmatrix} \in St(n, p)$$

is isomorphic to $O(n - p)$. We remind that the isotropy group for the identity frame X is a subgroup of $O(n)$ fixing X, i.e. $QX = X$ for any $Q \in O(n)$. Consequently, $\mathcal{M}$ is diffeomorphic to $O(n)/O(n - p)$ which turns the matrix manifold into a homogeneous space.

For any matrix representative $X \in \mathcal{M}$, the tangent space of $\mathcal{M}$ at X is defined as

$$T_X\mathcal{M} = \{Z \in \mathbb{R}^{n\times p} \mid X^T Z + Z^T X = 0\}.$$

Hence, the dimension of both $T_X\mathcal{M}$ and $\mathcal{M}$ is $np - p(p + 1)/2$. We can endow the Stiefel manifold with a different Riemannian metrics: the Euclidean metric and the canonical metric. In the two special cases when $p = 1$ and $p = n$, these two Riemannian metrics are equal. Otherwise they differ, and yield different formulas for geodesics and parallel translation. For

the purpose of this paper, we endow $\mathcal{M}$ with the canonical metric. In fact, let $X \in \mathcal{M}$, and $Z_1, Z_2 \in T_X\mathcal{M}$, then we define the canonical metric on $T_X\mathcal{M}$ by

$$\langle Z_1, Z_2 \rangle_X = \operatorname{trace}\left(Z_1^T \left(I_n - \frac{1}{2} X X^T \right) Z_2 \right). \tag{2.1}$$

Geodesics on a Riemannian manifold are locally shortest curves that are parametrized by the arc length. For a given curve $\gamma : [0,1] \to \mathcal{M}$, they satisfy the following second-order differential equation:

$$\ddot{\gamma} + \dot{\gamma}\dot{\gamma}^t\gamma + \gamma\big((\gamma^t\dot{\gamma})^2 + \dot{\gamma}^t\dot{\gamma}\big) = 0. \tag{2.2}$$

It is clear that this equation is numerically difficult to solve. Hopefully, the canonical structure allows a practical decomposition of the tangent space that simplify the characterization of geodesics.

Proposition 2.1. *Let X be a matrix representation on $\mathcal{M}$ and Z a tangent vector on $T_X M$. Then the geodesic $\gamma : [0,1] \to \mathcal{M}$ such that $\gamma(0) = X$ and $(\partial\gamma/\partial t)|_{t=0} = Z$ is given by*

$$\gamma(t) = XM(t) + QN(t), \tag{2.3}$$

where $M(t)$ and $N(t)$ are p-by-p matrices defined by

$$\begin{bmatrix} M(t) \\ N(t) \end{bmatrix} = \exp\left(t \begin{pmatrix} A & -R^t \\ R & 0 \end{pmatrix} \right) \begin{bmatrix} I_p \\ 0 \end{bmatrix}. \tag{2.4}$$

Proof. The proof starts with a decomposition of the tangent vector Z into its horizontal and vertical components with respect to the base point $X, Z = XX^TZ + (I_n - XX^T)Z$. Then, by letting $A = X^TZ$ a skew symmetric matrix and by means of a QR decomposition of $(I_n - XX^T)Z$, we get $Z = XA + QR$, which establishes the formula of the geodesic. □

Corollary 2.1. *Let $\gamma : [0,1] \to \mathcal{M}$ be a geodesic such that $\gamma(0) = X_1$ and $(\partial\gamma/\partial t)(t)|_{t=0} = Z \in T_{X_1}\mathcal{M}$. The Riemannian exponential map $\operatorname{Exp}_{X_1} : T_{X_1}\mathcal{M} \to \mathcal{M}$ that sends a Stiefel tangent vector Z to the endpoint $\gamma(1) = X_2$ is given by*

$$\operatorname{Exp}_{X_1}(Z) = X_1 M + QN = X_2 \in \mathcal{M}, \tag{2.5}$$

where M and N are the same as described in Eq. (2.4).

Conversely, given two points X_1 and $X_2 \in \mathcal{M}$, the inverse exponential map $\operatorname{Exp}_{X_1}^{-1}$ (also known as the logarithmic map Log_{X_1}) allows the recovery of the tangent vector $Z = \operatorname{Log}_{X_1}(X_2)$. Formulas to compute the Riemannian log map on the Stiefel manifold relative to the Euclidean metric are provided in [5,40]. As far as we know, until now, there exist two different approaches for evaluating the log map on the Stiefel manifold with respect to the canonical metric [34,43]. In this paper, we adopt the method provided in [43] and we suppose that each two points belong to a geodesic ball with an injectivity radius determined in [34].

Corollary 2.2. *The geodesic arc joining X_1 to X_2 in $\mathcal{M}$ can be parameterized explicitly by*

$$\gamma(t, X_1, X_2) = \operatorname{Exp}_{X_1}\big(t\operatorname{Log}_{X_1}(X_2)\big), \quad t \in [0,1]. \tag{2.6}$$

2.2. A Riemannian structure of the Grassmann manifold

The real Grassmann manifold $\mathcal{M} = G_{n,p}$ is defined as the set of p-dimensional $\mathbb{R}$-linear subspace of $\mathbb{R}^n$. It is a smooth and compact manifold of dimension $p(n-p)$. A point $\mathfrak{X} \in \mathcal{M}$ is a linear subspace that may be represented numerically as the span of a full-rank n-by-p matrix X

$$\mathcal{M} = \big\{\mathfrak{X} = \text{span}(X),\, X \in \mathbb{R}^{n\times p},\, \text{rank}(X) = p\big\}.$$

Remark 2.2. We can easily check that the matrix representative $X \in \mathfrak{X} \subset \mathcal{M}$ is a point on the Stiefel manifold $St(n,p)$. In particular, $\mathcal{M}$ is the quotient space of $St(n,p)$ by the action of the orthogonal Lie group $O(n)$, i.e. $\mathcal{M} = St(n,p)/O(p)$.

Definition 2.1. *For any $X \in \mathcal{M}$, the map $\varphi : \mathcal{M} \to \mathcal{M}$ defined by*

$$\varphi(X) = PXP^{-1}, \quad P = \begin{pmatrix} I_p & 0 \\ 0 & -I_{n-p} \end{pmatrix} \tag{2.7}$$

is an involutive automorphism, which turns the Grassmann manifold into a Riemannian symmetric space.

The symmetry φ will be an essential tools to handle the C^2 differentiability condition in $\mathcal{M}$. Given $X \in \mathcal{M}$, we identify the tangent space of $\mathcal{M}$ by

$$T_X\mathcal{M} = \big\{S \in \mathbb{R}^{n\times p} \mid X^T S = 0\big\}.$$

Unlike the case of the Stiefel manifold, introducing the metric based on the quotient space structure of $\mathcal{M}$ or that inherited from the Euclidean space $\mathbb{R}^{n\times n}$ on the tangent space $T_X\mathcal{M}$ conduct to the same metric. Hence, we will endow $\mathcal{M}$ with the one induced from the Frobenius inner product on $\mathbb{R}^{n\times n}$, for $S_1, S_2 \in T_X\mathcal{M}$, given by

$$\langle S_1, S_2\rangle_X = \text{tr}\big(S_1^T S_2\big).$$

Proposition 2.2. *Let A be a p-by-p skew-symmetric matrix and B an arbitrary $(n-p)$-by-p matrix. A geodesic $\gamma : [0,1] \to O(n)$ starting at $P \in O(n)$ in the direction of the tangent vector $P\left(\begin{smallmatrix} A & -B^t \\ B & O \end{smallmatrix}\right)$ lying on the horizontal space at P, is defined by*

$$\gamma(t) = P \exp\left(t \begin{pmatrix} A & -B^t \\ B & O \end{pmatrix}\right). \tag{2.8}$$

Then, geodesics in $\mathcal{M}$ are projections of the orthogonal Lie group $O(n)$ geodesics under the Riemannian submersion $\pi_1 : O(n) \to G_{n,p}$, that is a geodesic $\tilde{\gamma} : [0,1] \to G_{n,p}$ is given by $\tilde{\gamma}(t) = [\gamma(t)]$.

Corollary 2.3. *The exponential map $\text{Exp}_X : T_X\mathcal{M} \to \mathcal{M}$ is defined as*

$$\text{Exp}_X(S) = \big(XW\cos(\Sigma) + V\sin(\Sigma)\big)W^t, \tag{2.9}$$

where $(V\Sigma W^t)$ is the compact singular value decomposition of the tangent vector $S \in T_X\mathcal{M}$.

Gallivan *et al.* [24] have proposed a method to compute the inverse of the exponential map which is based on the representation of $\mathcal{M}$ with $SO(n)/(SO(p)\times SO(n-p))$ and some results from linear algebra, the CS (cosine-sine) decomposition in particular.

Proposition 2.3. *Let X_1 and $X_2 \in \mathcal{M}$. The log-map $\mathrm{Log}_{X_1}(X_2) : \mathcal{M} \to T_{X_1}\mathcal{M}$ is defined as*

$$\mathrm{Log}_{X_1}(X_2) = W_2 \Sigma W_1^t, \tag{2.10}$$

where W_2, W_1 are given by the CS decomposition

$$\begin{bmatrix} X_1^t X_2 \\ \big(I_n - X_1 X_1^t\big) X_2 \end{bmatrix} = \begin{bmatrix} W_1 \cos(\Sigma) V^t \\ W_2 \sin(\Sigma) V^t \end{bmatrix}. \tag{2.11}$$

Corollary 2.4. *The shortest geodesic arc joining X_1 to X_2 in $\mathcal{M}$ is given by*

$$\gamma(t, X_1, X_2) = \mathrm{Exp}_{X_1}\left(t \mathrm{Log}_{X_1}(X_2)\right), \quad t \in [0,1]. \tag{2.12}$$

Here and subsequently,

$$\dot{\gamma}(t, X_1, X_2) := \frac{\partial}{\partial u}\Big|_{u=t} \gamma(u, X_1, X_2), \tag{2.13}$$

and $(d\mathrm{Exp}_{X_1})_S$ stands for the derivative of Exp_{X_1} at $S \in T_{X_1}\mathcal{M}$.

3. C^1 Interpolation on the Stiefel Manifold $\mathcal{M} = St(n,p)$

In this section, we introduce a method to construct a C^1 interpolating Bézier spline for smoothing data that are constrained to live in the Stiefel Manifold $\mathcal{M}$ equipped with its canonical Riemannian metric. More explicitly, consider $(N+1)$ distinct data points $X_0, \cdots, X_N$ in $\mathcal{M}$ associated with time instants $t_i = i, i = 0, \ldots, N$. Our goal is to estimate a spline $\alpha : [0, N] \to \mathcal{M}$, minimizing the cost functional (1.1), and satisfying the following properties:

(i) $\alpha(t_i) = X_i,\ i = 0, \ldots, N.$

(ii) α is conformed by N Bézier curves of order j.

(iii) α is of class C^1.

Let us recall that geometrically a Bézier curve of order j in the Euclidean space $\mathbb{R}^n$ is a polynomial function defined by a sequence of control points expressed in a particular basis called the Bernstein basis polynomials such that the first and last control points of the curve are interpolated but the intermediate control points are in general not on the curve. A simple algorithm to construct such curve is called De Casteljau algorithm and is based only on a successive linear interpolation [11]. Therefore, one idea to define a Bézier curve of order j on Riemannian manifolds is to generalize the De Casteljau's algorithm. It can be easily seen that by replacing straight lines by minimal geodesic between two points, the generalization of the De Casteljau's algorithm is made in an obvious way.

Definition 3.1. *The Bézier curve $\alpha_j : [0, N] \to \mathcal{M}, t \to \alpha_j(t; V_0, \cdots, V_j)$ of order j parametrized by $(j+1)$ control points $V_0, \cdots, V_j$ is defined as follows. Consider the point $V_i^0 = V_i$ and we iterate the construction of further points. In fact, for $i = 0, \ldots, j-k$, $k = 1, \ldots, j$,*

$$V_i^k = \alpha_k(t, V_i, \cdots, V_{i+k}) = \mathrm{Exp}_{V_i^{k-1}}\left(t \mathrm{Log}_{V_i^{k-1}}\big(V_{i+1}^{k-1}\big)\right), \quad t \in [0,1]$$

represent the i-th point of the k-th step of the De Casteljau algorithm, and thus

$$\alpha_j(t; V_0, \cdots, V_j) = V_0^j.$$

The resulting Bézier spline $\alpha : [0, N] \to \mathcal{M}$ is only formed by a sequence of N Bézier curves $\alpha_j^i, j \in \{2, 3\}$ and $i = 0, \ldots, N-1$ such that first and last ones are quadratic Bézier curves while all the others are cubic.

Definition 3.2. *Assume that there exists two artificial control points* $(\widehat{Y}_i^-, \widehat{Y}_i^+)$ *on the left- and on the right-hand side of the interpolation point* X_i, $i = 1, \ldots, N-1$ *defining a chain of Bézier curve* $\alpha_j^i, j \in \{2,3\}, 0 \leq i \leq N-1$. *The Bézier spline* $\alpha : [0, N] \longrightarrow \mathcal{M}$ *is then given by*

$$\alpha(t) = \begin{cases} \alpha_2^0\big(t; X_0, \widehat{Y}_1^-, X_1\big), & 0 \leq t \leq 1, \\ \alpha_3^i\big(t-i; X_i, \widehat{Y}_i^+, \widehat{Y}_{i+1}^-, X_{i+1}\big), & i-1 \leq t \leq i, \\ \alpha_2^{N-1}\big(t-(N-1); X_{N-1}, \widehat{Y}_{N-1}^+, X_N\big), & N-1 \leq t \leq N. \end{cases}$$

As the Bézier spline α interpolates the first and the last control points of each Bézier curve $\alpha_j^i, j \in \{2,3\}, 0 \leq i \leq N-1$, we are left with the task of determining the remaining control points $(\widehat{Y}_i^-, \widehat{Y}_i^+), i = 0, \ldots, N-1$. Note that we want α to be at least C^1. It is immediate, by construction, that the spline α is C^∞ on $]t_i, t_{i+1}[$, $i = 1, \ldots, N-1$. We are thus looking to ensure the differentiability condition at the knot points. Our main idea to handle this issue is to treat the fitting problem on different tangent space. Specifically, let $X_0, \cdots, X_N$ be a set of distinct given points in $\mathcal{M}$ with X_l being in the cut locus of $X_i, i \neq l$. The cut locus of X_l in $\mathcal{M}$, in turn, is the set of points in $\mathcal{M}$ where the geodesics starting at X_l stop being length-minimizing. By means of the algorithm of the logarithm map developed in [34, 43] for Stiefel manifold, we transport data points $X_0, \cdots, X_N$ to $T_{X_i}\mathcal{M}$ at a point $X_i \in \mathcal{M}, i = 1, \ldots, N-1$. Let us denote the mapped data by $Z^i = (Z_0^i, \cdots, Z_N^i)$ with $Z_m^i = \mathrm{Log}_{X_i}(Z_m)$ for $m = 0, \ldots, N$. Now our next concern is to search for the control points of a C^1 Bézier spline on $T_{X_i}\mathcal{M}, i = 1, \ldots, N-1$.

From this tangential solution, the Riemannian exponential map Exp_{X_i} defined on $\mathcal{M}$ by Eq. (2.5) will bring back the solution to the matrix manifold $\mathcal{M}$. The resulting Bézier spline α is then reconstructed with De Casteljau algorithm and we prove that is optimal. So let $\beta : [0, N] \to T_{X_i}\mathcal{M}$ denote the Bézier spline on $T_{X_i}\mathcal{M}, i = 1, \ldots, N-1$ defined identically to the Bézier spline on $\mathcal{M}$ by N Bézier curves $\beta_k^i, k \in \{2,3\}, 0 \leq i \leq N-1$. And let $(B_m^i)^-$ and $(B_m^i)^+$ denote control points on the left- and on the right-hand side of the interpolation point Z_m for $m = 1, \ldots, N-1$. Hence,

$$\beta(t) = \begin{cases} \beta_2^0\big(t; Z_0^i, (B_1^i)^-, Z_1^i\big), & 0 \leq t \leq 1, \\ \beta_3^i\big(t-i; Z_i^i, (B_i^i)^+, (B_{i+1}^i)^-, Z_{i+1}^i\big), & i-1 \leq t \leq i, \\ \beta_2^{N-1}\big(t-(N-1); Z_{N-1}^i, \big(B_{N-1}^i\big)^+, Z_N^i\big), & N-1 \leq t \leq N. \end{cases}$$

Proposition 3.1. *The optimization problem Eq.* (1.1)*, which is not easy to solve directly on* $\mathcal{M}$ *is simplified to an Euclidean cost function on* $T_{X_i}\mathcal{M}, i = 1, \ldots, N-1$*, given by*

$$\begin{aligned} \min_{(B_1^i)^-, \cdots, (B_{N-1}^i)^-} & E\big(\big(B_1^i\big)^-, \cdots, \big(B_{N-1}^i\big)^-\big) \\ := & \min_{(B_1^i)^-, \cdots, (B_{N-1}^i)^-} \int_0^1 \big\|\ddot{\beta}_2^0\big(t; Z_0^i, \big(B_1^i\big)^-, Z_1^i\big)\big\|^2 \\ & + \sum_{m=1}^{N-2} \int_0^1 \big\|\ddot{\beta}_3^i\big(t; Z_m^i, \big(B_m^i\big)^+, \big(B_{m+1}^i\big)^+, Z_{m+1}^i\big)\big\|^2 \\ & + \int_0^1 \big\|\ddot{\beta}_2^{N-1}\big(t; Z_{N-1}, \big(B_{N-1}^i\big)^+, Z_N^i\big)\big\|^2, \end{aligned} \tag{3.1}$$

where $\|.\|$ *represents the canonical norm on the tangent space* $T_{X_i}\mathcal{M}, i = 1, \ldots, N$.

Proof. We give the proof only for the case $i = 1$, the other ones being similar. Let $X_0, \cdots, X_N$ a set of $(N+1)$ data points in $\mathcal{M}$ and $Z^1 = (Z_0^1, \cdots, Z_N^1)$ their corresponding mapped data in the tangent space $T_{X_1}\mathcal{M}$. Let $t \longrightarrow \beta_k(t; B_0^1, \cdots, B_N^1)$ denote the Bézier curve of order $k \in \{2, 3\}$ in $T_{X_1}\mathcal{M}$ defined with its control points $B_0^1, \cdots, B_N^1$ in the Bernstein basis polynomials of degree k as

$$\begin{aligned}\beta_2\big(t; B_0^1, B_1^1, B_2^1\big) &= B_0^1(1-t)^2 + 2B_1^1(1-t)t + B_2^1 t^2,\\ \beta_3\big(t; B_0^1, B_1^1, B_2^1, B_3^1\big) &= B_0^1(1-t)^3 + 3B_1^1 t(1-t)^2 + 3B_2^1 t^2(1-t) + B_3^1 t^3.\end{aligned} \tag{3.2}$$

Let $((B_m^1)^-, (B_m^1)^+)$ denote the two control points on the left- and the right-hand side of the interpolation point Z_m^1, $m = 1, \ldots, N-1$. Furthermore, to ensure that β is C^1, we shall make the following assumption:

$$\begin{aligned}&\dot\beta_{k^i}\big(\big(B_0^1\big)^i, \cdots, \big(B_{k^i}^1\big)^i; t-i+1\big)\big|_{t=i}\\ &= \dot\beta_{k^{i+1}}\big(\big(B_0^1\big)^{i+1}, \cdots, \big(B_{k^{i+1}}^1\big)^{i+1}; t-i\big)\big|_{t=i}, \quad i = 0, \ldots, N-2.\end{aligned} \tag{3.3}$$

This differentiability condition allows us to express $(B_m^1)^-$ in terms of $(B_m^1)^+$ as

$$\big(B_1^1\big)^+ = \frac{5}{3}Z_1^1 - \frac{2}{3}\big(B_1^1\big)^-, \tag{3.4}$$

$$\big(B_i^1\big)^+ = 2Z_i^1 - \big(B_i^1\big)^-, \quad i = 2, \ldots, N-2, \tag{3.5}$$

$$\big(B_{N-1}^1\big)^+ = \frac{5}{2}Z_{N-1}^1 - \frac{3}{2}\big(B_{N-1}^1\big)^-. \tag{3.6}$$

Hence, the task now is reduced to search only control points $(B_i^1)^-$, $i = 1, \ldots, N-1$, that generate the C^1 Bézier spline β in $T_{X_1}\mathcal{M}$. Replacing the new optimization variables in problem (1.1) gives

$$\begin{aligned}&\min_{(B_1^1)^-, \cdots, (B_{N-1}^1)^-} E\big(\big(B_1^1\big)^-, \cdots, \big(B_{N-1}^1\big)^-\big)\\ &\qquad := \min_{(B_1^1)^-, \cdots, (B_{N-1}^1)^-} \int_0^1 \big\|\ddot\beta_2^0\big(t; Z_0^1, \big(B_1^1\big)^-, Z_1^1\big)\big\|^2\\ &\qquad\quad + \sum_{m=1}^{N-2}\int_0^1 \big\|\ddot\beta_3^i\big(t; Z_m^1, \big(B_m^1\big)^+, \big(B_{m+1}^1\big)^+, Z_{m+1}^1\big)\big\|^2\\ &\qquad\quad + \int_0^1 \big\|\ddot\beta_2^{N-1}\big(t; Z_{N-1}, \big(B_{N-1}^1\big)^+, Z_N^1\big)\big\|^2,\end{aligned} \tag{3.7}$$

which is merely the problem of minimization of the mean square acceleration of the Bézier curve β in the Euclidean space $\mathbb{R}^n$. □

The problem (3.1) is now treated similarly as the Euclidean case $\mathcal{M} = \mathbb{R}^n$. Actually, we prove that solutions of the mean square acceleration are exactly the control points of β. Details of the solution of (3.1) on $\mathbb{R}^n$ are given in Appendix A. Furthermore, we give a geometrical illustration of our approach in Fig. 3.1.

Theorem 3.1. *Given $X_0, \cdots, X_N$ a set of $(N+1)$ data points in $\mathcal{M}$ and $B^i = [(B_1^i)^-, \cdots, (B_{N-1}^i)^-]^T$ a matrix of size $(n(N-1)\times n)$ containing the $(N-1)$ control points that generate β_i in each tangent space $T_{X_i}\mathcal{M}$, $i = 1, \ldots, N-1$. Then, the Bézier spline $\alpha : [0, N] \to \mathcal{M}$*

interpolating the data points X_i on $\mathcal{M}$ is of class C^1 and is uniquely defined by the set of control points $Y = [\widehat{Y}_1^-, \cdots, \widehat{Y}_{N-1}^-]^T \in \mathbb{R}^{n(N-1)\times n}$ where the rows of $\widehat{Y}$ are given by

$$\widehat{Y}_i^- = \mathrm{Exp}_{X_i}\big((B_i^i)^-\big), \quad i = 1, \ldots, N-1. \tag{3.8}$$

Proof. To solve the optimization problem (3.1), we need to compute the critical points of the gradient of the energy function E. Again, we give the proof for the case $i = 1$. Let us first examine the inner product of the acceleration. In fact, the acceleration on respective intervals is given by

$$\begin{aligned}
&\ddot{\beta}_2\big(t; B_0^1, B_1^1, B_2^1\big) = 2B_0^1 - 4B_1^1 + 2B_2^1,\\
&\ddot{\beta}_3\big(t; B_0^1, B_1^1, g_2^1, B_3^1\big) = 6B_0^1 - 12B_1^1 + 6B_2^1 + 6t\big(-B_0^1 + 3B_1^1 - 3B_2^1 + B_3^1\big).
\end{aligned} \tag{3.9}$$

Then we compute the inner product of the acceleration with respect to the inner product defined in $T_{X_1}\mathcal{M}$, we thus get

$$\begin{aligned}
\|\ddot{\beta}_2\|^2 &= 4\big(\langle B_0^1, B_0^1\rangle - 4\langle B_0^1, B_1^1\rangle + 2\langle B_0^1, B_2^1\rangle + 4\langle B_1^1, B_1^1\rangle\\
&\quad - 4\langle B_2^1, B_1^1\rangle + \langle B_2^1, B_2^1\rangle\big),\\
\|\ddot{\beta}_3\|^2 &= 36\big\langle B_0^1 - 2B_1^1 + B_2^1 + t\big(-B_0^1 + 3B_1^1 - 3B_2^1 + B_3^1\big),\\
&\quad B_0^1 - 2B_1^1 + B_2^1 + t\big(-B_0^1 + 3B_1^1 - 3B_2^1 + B_3^1\big)\big\rangle.
\end{aligned}$$

Finally, we evaluate the integral of each term of Eq. (3.7), we obtain

$$\begin{aligned}
\int_0^1 \|\ddot{\beta}_2\|^2 dt = \|\ddot{\beta}_2\|^2 &= 4\big(\langle B_0^1, B_0^1\rangle - 4\langle B_0^1, B_1^1\rangle + 2\langle B_0^1, B_2^1\rangle\\
&\quad + 4\langle B_1^1, B_1^1\rangle - 4\langle B_2^1, B_1^1\rangle + \langle B_2^1, B_2^1\rangle\big),\\
\int_0^1 \|\ddot{\beta}_3\|^2 dt = 36\Big(&\frac{1}{3}\langle B_0^1, B_0^1\rangle - \langle B_0^1, B_1^1\rangle + \frac{1}{3}\langle B_0^1, B_3^1\rangle + \langle B_1^1, B_1^1\rangle\\
&- \langle B_1^1, B_2^1\rangle + \langle B_2^1, B_2^1\rangle - \langle B_2^1, B_3^1\rangle + \frac{1}{3}\langle B_3^1, B_3^1\rangle\Big).
\end{aligned}$$

By replacing B_k^1 such that $B_0^1 = Z_0^1, B_1^1 = (B_1^1)^-$ and $B_2^1 = Z_1^1$ for the first interval, $B_0^1 = Z_{N-1}^1$, $B_1^1 = (B_{N-1}^1)^-$ and $B_2^1 = Z_N^1$ for the last interval, and $B_0^1 = Z_k^1, B_1^1 = (B_k^1)^+, B_2^1 = (B_{k+1}^1)^-$

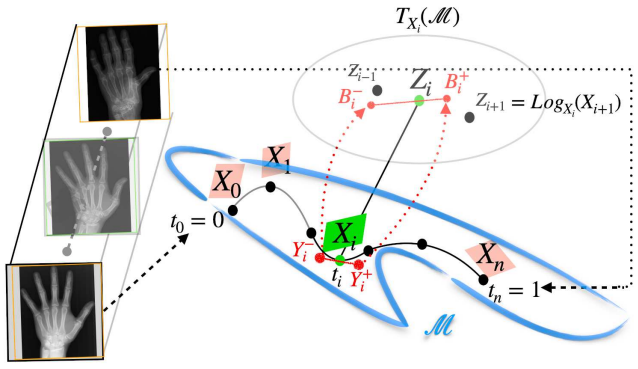

Fig. 3.1. Geometrical illustration of the Riemannian manifold $\mathcal{M}$ and its tangent space $T_{X_i}\mathcal{M}$ at $X_i \in \mathcal{M}$. γ is an interpolating spline with $X_t = \gamma(t)$ for $t \in I$ which verifies $\gamma(t)^T\gamma(t) = I_p$ for all $t \in I$.

and $B_3^1 = Z_{k+1}^1$ for the intermediate intervals, it leads to the apparition of constant terms K involving all Z_k^1 which will disappear when we derive the gradient. As detailed in Appendix A, the new formulation becomes

$$\begin{aligned}
&\min_{(B_1^1)^-,\cdots,(B_{N-1}^1)^-} E\big((B_1^1)^-,\cdots,(B_{N-1}^1)^-\big)\\
&\quad= 4\Big(-4\big\langle Z_0^1,(B_1^1)^-\big\rangle + 4\big\langle (B_1^1)^-,(B_1^1)^-\big\rangle - 4\big\langle Z_0^1,(B_1^1)^-\big\rangle\Big)\\
&\qquad+\sum_{k=1}^{N-2} 36\Big(-\big\langle Z_k^1,(B_k^1)^+\big\rangle + \big\langle (B_k^1)^+,(B_k^1)^+\big\rangle - \big\langle (B_k^1)^+,(B_{k+1}^1)^-\big\rangle\\
&\qquad\qquad+\big\langle (B_{k+1}^1)^-,(B_{k+1}^1)^-\big\rangle - \big\langle (B_{k+1}^1)^-,Z_{k+1}^1\big\rangle\Big)\\
&\qquad+4\Big(-4\big\langle Z_{N-1}^1,(B_{N-1}^1)^+\big\rangle + 4\big\langle (B_{N-1}^1)^+,(B_{N-1}^1)^+\big\rangle - 4\big\langle Z_N^1,(B_{N-1}^1)^+\big\rangle\Big) + K.
\end{aligned}$$

After changing $(B_k^1)^+$'s by $(B_k^1)^-$'s using Appendix A, the next step is to compute the gradient and search for the optimal solution $(B_k^1)^-$. Consequently, $\forall w \in T_{X_1}\mathcal{M}$ the optimal solution is given by

$$\begin{aligned}
\frac{\partial E}{\partial (B_1^1)^-} &= 4\Big(8\big\langle (B_1^1)^-,w\big\rangle - 4\big\langle Z_0^1,w\big\rangle - 4\big\langle Z_1^1,w\big\rangle\Big)\\
&\quad+36\Big(-\frac{14}{9}\big\langle Z_1^1,w\big\rangle + \frac{8}{9}\big\langle (B_1^1)^-,w\big\rangle + \frac{6}{9}\big\langle (B_2^1)^-,w\big\rangle\Big) = 0,\\
\frac{\partial E}{\partial (B_2^1)^-} &= 36\Big(-\frac{5}{3}\big\langle Z_1^1,w\big\rangle + \frac{2}{3}\big\langle (B_1^1)^-,w\big\rangle + 2\big\langle (B_2^1)^-,w\big\rangle - \big\langle Z_2^1,w\big\rangle\Big)\\
&\quad+36\Big(-3\big\langle Z_2^1,w\big\rangle + 2\big\langle (B_2^1)^-,w\big\rangle + \big\langle (B_3^1)^-,w\big\rangle\Big) = 0,\\
\frac{\partial E}{\partial (B_k^1)^-} &= 36\Big(-3\big\langle Z_j^1,w\big\rangle + 2\big\langle (B_j^1)^-,w\big\rangle + \big\langle (B_{j+1}^1)^-,w\big\rangle\Big)\\
&\quad+36\Big(-2\big\langle Z_{j-1}^1,w\big\rangle + \big\langle (B_{j-1}^1)^-,w\big\rangle\\
&\qquad+2\big\langle (B_{j-1}^1)^-,w\big\rangle - \big\langle Z_j^1,w\big\rangle\Big) = 0,\quad j=2,\ldots,N-2,\\
\frac{\partial E}{\partial (B_{N-1}^1)^-} &= 36\Big(-2\big\langle Z_{N-2}^1,w\big\rangle + \big\langle (B_{N-2}^1)^-,w\big\rangle + 2\big\langle (g_{N-1}^1)^-,w\big\rangle - \big\langle Z_{N-1}^1,w\big\rangle\Big)\\
&\quad+4\Big(-24\big\langle Z_{N-1}^1,w\big\rangle + 18\big\langle (B_{N-1}^1)^-,w\big\rangle + 6\big\langle Z_N^1,w\big\rangle\Big) = 0.
\end{aligned} \tag{3.10}$$

Consequently, similar as the Euclidean case $\mathbb{R}^n$, the solution of Eq. (3.1) is given by

$$B^1 = \big[(B_1^1)^-,\cdots,(B_{N-1}^1)^-\big]^T = D\tilde{P},$$

and therefore, $\widehat{Y}_1^- = \exp_{X_1}(\tilde{x}_1)$ where

$$\tilde{x}_1 = (B_1^1)^- = \sum_{k=0}^{n} D_{1k} X_k^1.$$

The differentiability condition at the interpolation points allows us to express control points $(B_1^i)^-$ in terms of $(B_1^i)^+$ as

$$(B_1^i)^- = X_i + \lambda_i\big((B_1^i)^+ - X_i\big). \tag{3.11}$$

Considering that $\log_p(b) = b - p$ in the Euclidean case, hence the generalization of Eq. (3.11) on $\mathcal{M}$ is given by

$$\widehat{Y}_i^+ = \mathrm{Exp}_{X_i}\Big(\lambda_i \mathrm{Exp}_{X_i}^{-1}\big(\widehat{Y}_i^-\big)\Big), \tag{3.12}$$

which assert the C^1 differentiability condition on $\mathcal{M}$. □

Algorithm 3.1 synthesizes all steps needed to construct the C^1 solution on $\mathcal{M}$.

Algorithm 3.1: C^1 Solution on the Stiefel manifold $\mathcal{M}$.

Input : $N \geq 3$, $(X_0, \cdots, X_N)$ a matrix of size $N(n+1) \times N$ containing the $(N+1)$ interpolation points on $\mathcal{M}$.
Output: $\widehat{Y}$.

for $i = 1 : N-1$ **do**
  Compute $Z = [Z_0^i, \cdots, Z_N^i]^T$ a matrix of size $N(n+1) \times N$ containing the $(N+1)$ interpolation points on $T_{X_i}\mathcal{M}$.
  for $k = 0 : N$ **do**
    $Z_k^i = \mathrm{Log}_{X_i}(X_k)$.
    Compute $B^i = [(B_1^i)^-, \cdots, (B_{N-1}^i)^-]^T$ a matrix of size $N(n-1) \times N$ containing the $(N-1)$ control points of the C^1 Bézier curve β_i on $T_{X_i}\mathcal{M}$, using Appendix A.
    Compute control point $\widehat{Y}_i^- = \mathrm{Exp}_{X_i}((\widehat{B}_i^i)^-)$ on $\mathcal{M}$.
  end
end
return $\widehat{Y}$.

4. C^2 Interpolation on the Grassmann Manifold $\mathcal{M} = G_{n,p}$

In this section, we will show that in the case of the Grassmann Manifold $\mathcal{M}$, the Bézier spline α is of class C^2 due to the elegant properties of this manifold. In other words, we are again given $(N+1)$ distinct data points $X_0, \cdots, X_N$ in $\mathcal{M}$ associated with time instants $t_i = i, i = 0, \ldots, N$. Our goal is to construct a Bézier spline $\alpha : [0, N] \to \mathcal{M}$ interpolating the data points X_i, $i = 0, \ldots, N$ and assuring a C^2 differentiability condition at the knot points. Similarly as in the previous section, the Bézier spline α will be constructed recursively by a chain of Bézier curve α_j, $j \in \{2, 3\}$ defined by a set of $(N-1)$ control points $(\widehat{Y}_i^-, \widehat{Y}_i^+)$ on the left- and on the right-hand side of the interpolation point X_i, $i = 1, \ldots, N-1$. Our algorithm to find optimal control points of the C^2 Bézier spline in $\mathcal{M}$ consists of the following two phases:

Phase 1: We construct an interpolation Bézier spline $\alpha : [0, N] \to \mathcal{M}$ in $\mathcal{M}$ only C^1. To do these, for each $i = 1, \ldots, N-1$, we transfer the data $X_0, \cdots, X_N$ in each tangent space $T_{X_i}\mathcal{M}$ using Riemannian logarithmic map given by (2.10). The mapped data are then given by $S^i = (S_0^i, \cdots, S_N^i)$ with $S_k^i = \mathrm{Log}_{X_i}(X_k)$ for $k = 0, \ldots, N$, and $i = 1, \ldots, N-1$. Then, by means of equations that govern the control points of the C^2 Bézier spline on $\mathbb{R}^n$ given in Appendix A, we construct the C^2 Bézier curve β_i in each tangent space $T_{X_i}\mathcal{M}$, $i = 1, \ldots, N-1$. Finally, the Riemannian exponential map Exp_{X_i} defined on $\mathcal{M}$ by (2.9) will transport control points of the C^2 Bézier curve β_i from the tangent space $T_{X_i}\mathcal{M}$ to the matrix manifold $\mathcal{M}$ which

provides control point of the desired C^1 interpolation Bézier spline α in $\mathcal{M}$. We summarize this result in Theorem 4.1.

Theorem 4.1. *Given $X_0, \cdots, X_N$ a set of $(N+1)$ points in $\mathcal{M}$, and $B^i = [(B_1^i)^-, \cdots, (B_{N-1}^i)^-]^T$ a matrix of size $(n(N-1) \times n)$ such that each row $\tilde{x}_i$ of B^i contains optimal control points of the C^2 Bézier spline β_i in each tangent space $T_{X_i}\mathcal{M}$, $i = 1, \ldots, N-1$. Then, the Bézier spline $\alpha : [0, N] \to \mathcal{M}$ interpolating the data X_i is of class C^1 and is uniquely defined by the set of control points $\widehat{Y} = [\widehat{Y}_1^-, \cdots, \widehat{Y}_{N-1}^-]^T \in \mathbb{R}^{n(N-1)\times n}$ given by*

$$\widehat{Y}_i^- = \mathrm{Exp}_{X_i}(\tilde{x}_i), \quad i = 1, \ldots, N-1. \tag{4.1}$$

Proof. The proof is similar to the one of Theorem 3.1. □

Remark 4.1. The interpolation point X_N is modified under the C^2 differentiability condition of the curve β_i on $T_{X_i}\mathcal{M}$, $i = 1, \ldots, N-1$, therefore the point X_N is changed and the new $(N+1)$ interpolation points on $\mathcal{M}$ is given by

$$\tilde{X}_k = \mathrm{Exp}_{Xi}(\tilde{S}_k^i), \quad k = 0, \ldots, N, \quad i = 1, \ldots, N-1, \tag{4.2}$$

where $\tilde{S} = [\tilde{S}_0^i, \cdots, \tilde{S}_N^i]^T$ a matrix of size $n(N+1)\times n$ containing the new $(N+1)$ interpolation points in each tangent space $T_{X_i}\mathcal{M}$. More details are given in Appendix A.

It is important to notice that at this first step, the Bézier spline α is only of class C^1. Our next goal is to show how to arrange α to satisfy the C^2 differentiability condition at points X_i, $i = 1, \ldots, N$.

Phase 2: At this step, nice properties of symmetric spaces are involves. Lemma B.1 and Theorem B.1 in Appendix B examine in details the relation made between global symmetries at interpolation points and the C^2 differentiability of the Bézier spline on symmetric spaces. In fact, this requires the computation of the derivative of the geodesic symmetry given by Eq. (2.7) and the derivative of the Riemannian exponential map Exp_{X_i} defined in $\mathcal{M}$ by (2.9). Let us denote by Y_i^- and Y_i^+ the new control points on the left- and on the right-hand side of the interpolation point $\tilde{X}_i$ that define the Bézier spline α in $\mathcal{M}$. Our basic idea to find control points Y_i^-, $i = 1, \ldots, N-1$ is similar to the Euclidean case $\mathbb{R}^n$. That is, we might know Y_1^- (and therefore Y_1^+ by the C^1 differentiability condition in $\mathcal{M}$) and wish to define iteratively Y_i^-, $i = 2, \ldots, N-1$ (and obviously Y_i^+ in much the same way as Y_1^+).

Theorem 4.2. *Under the hypotheses of Theorem 4.1, the Bézier spline $\alpha : [0, N] \to M$ is C^2 and is uniquely defined by the set of control points given by the row of the matrix $Y = [Y_1^-, \cdots, Y_{N-1}^-]^T \in \mathbb{R}^{n(N-1)\times n}$ by*

1. $Y_1^- = \mathrm{Exp}_{\tilde{X}_1}((\widehat{B}_1^1)^-)$,
2. $Y_2^- = \mathrm{Exp}_{Y_1^+}\big(((d\varphi_{\tilde{X}_1})_{Y_1^-}(\dot{\gamma}(1, \tilde{X}_0, Y_1^-)) - 4\dot{\gamma}(0, Y_1^-, \tilde{X}_1))/3\big)$,
3. $Y_{i+1}^- = \mathrm{Exp}_{Y_i^+}\big(((d\varphi_{\tilde{X}_i})_{Y_i^-}(\dot{\gamma}(1, Y_{i-1}^+, Y_i^-)) - 2\dot{\gamma}(0, Y_i^-, \tilde{X}_i))\big)$, $i = 2, \ldots, N-2$,

where $d\varphi_{\tilde{X}_i}$ represent the derivative of the symmetry map $\varphi_{\tilde{X}_i}$ at a point $Y_i^-, i = 1, \ldots, N-1$.

Proof. The proof strongly depends on the results given in [33]. Hence, all technical details of the proof will be given in Appendix B. For convenience, we remind the main ideas:

1. In [33], they compute the covariant derivative of a tangent vector along a curve and provide the explicit C^2 condition on symmetric spaces in terms of the derivative of exponential and symmetry functions. We make use of this result and Theorem 3.1 to simplify the derivative of the inverse of the exponential map.

2. We express the derivative of the symmetry as a function of the tangent vector along the Bézier spline α_i^j at $t = 0$ and $t = 1$ which simplify the C^2 condition in [33] and help us to obtain an explicit expression for control points that generate the Bézier spline α.

We summarize the different steps of the proof in Algorithm 4.1.

Algorithm 4.1: C^2 interpolating Bézier spline on the Grassmann manifold $\mathcal{M}$.

Input : $N \geq 3$, $\tilde{X} = [\tilde{X}_0, \cdots, \tilde{X}_N]^T$ a matrix of size $n(N+1) \times n$ containing the $(N+1)$ interpolation points in $\mathcal{M}$.

Output: Y.

Calculate $\widehat{Y} = [\widehat{Y}_1^-, \cdots, \widehat{Y}_{N-1}^-]^T$ a matrix of size $n(N-1) \times n$ containing the $(N-1)$ control points of the C^2 Bézier curve β_i on $T_{X_i}\mathcal{M}$ using Appendix A.

Set $Y_1^- = \widehat{Y}_1^-$.

Calculate control point Y_1^+:

$Y_1^+ = \mathrm{Exp}_{\tilde{X}_1}(-(2/3)\mathrm{Exp}^{-1}_{\tilde{X}_1}(Y_1^-))$.

Calculate control point Y_2^-:

$Y_2^- = \mathrm{Exp}_{Y_1^+}(((d\varphi_{\tilde{X}_1})_{Y_1^-}(\dot{\gamma}(1, \tilde{X}_0, Y_1^-)) - 4\dot{\gamma}(0, Y_1^-, \tilde{Y}_1))/3)$.

for $i = 2 : N-2$ **do**

  $Y_i^+ = \mathrm{Exp}_{\tilde{X}_i}(-\mathrm{Exp}^{-1}_{\tilde{X}_1}(Y_i^-))$.

  $Y_{i+1}^- = \mathrm{Exp}_{Y_i^+}((d\varphi_{\tilde{X}_i})_{Y_i^-}(\dot{\gamma}(1, Y_{i-1}^+, Y_i^-)) - 2\dot{\gamma}(0, Y_i^-, \tilde{X}_i))$.

end

Calculate control point Y_{N-1}^+:

$Y_{N-1}^+ = \mathrm{Exp}_{\tilde{X}_{N-1}}(-(2/3)\mathrm{Exp}^{-1}_{\tilde{X}_{N-1}}(Y_{N-1}^-))$.

return Y.

The proof is complete. □

5. Experiments

We consider numerical and real-world examples where data points $X_0, X_1, \cdots, X_N$ on a manifold $\mathcal{M}$ are not necessarily parametric. So we can not restrict applications to a class of X_i. We display some examples of random points on a Stiefel manifold $\mathcal{M}$ in Fig. 5.1. For each point X_i, we plot the components $(X_i[1]), (X_i[2])$ and $(X_i[3])$ in blue, green and red, respectively. The coordinates are then connected with edges to show the shape of the triangle. This illustration outlines how the positions (components) change and how the shape of the triangle evolves from one point to another. We also note that those points are random inside a geodesic ball so that all the properties detailed in the previous sections are satisfied in order to define an interpolating spline between them. Examples are random and different which capture large variability

for illustration. Moreover, Fig. 5.2 shows examples from real-world data. We can observe that the numerical examples, even random, provide good candidates for tests.

In the rest of this section, we illustrate the performance of the proposed method via different experiments. In all cases, we have considered a finite set of data points $X_0, X_1, \cdots, X_N$ on a Stiefel manifold $\mathcal{M}$. Each data point X_i is given at a fixed time instant t_i with $i = 0, 1, \ldots, N$ and $(t_0, t_N) = (0, 1)$, for simplicity. In the first setting, we consider a very common situation where data points are elements on $St(n, 1) = S^{n-1}$. This situation is standard in many applications. To cite but a few popular ones: Normalized directions, longitudinal data, and rotations which is equivalent to $SO(n)$. In the second regression setting, we consider another example where data points are elements on $St(n, p)$ with $p = 2$ and $n = 3$.

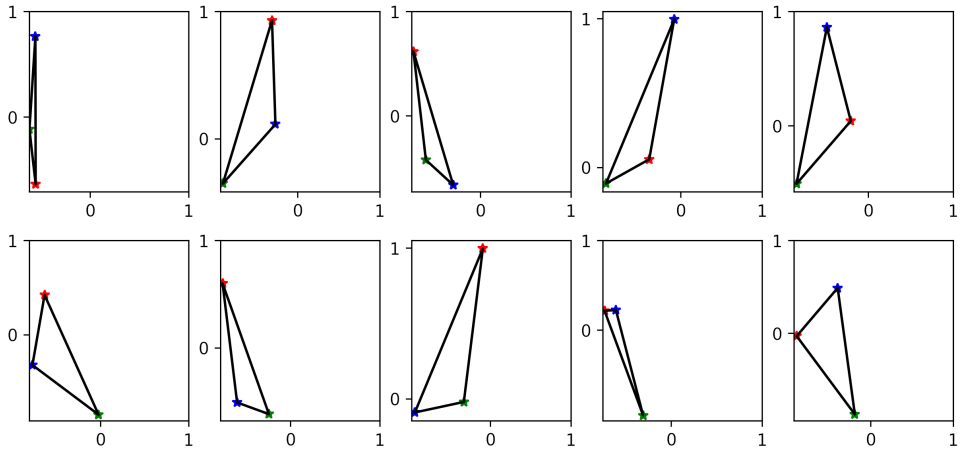

Fig. 5.1. Random numerical examples on $\mathcal{M} = St(3, 2)$.

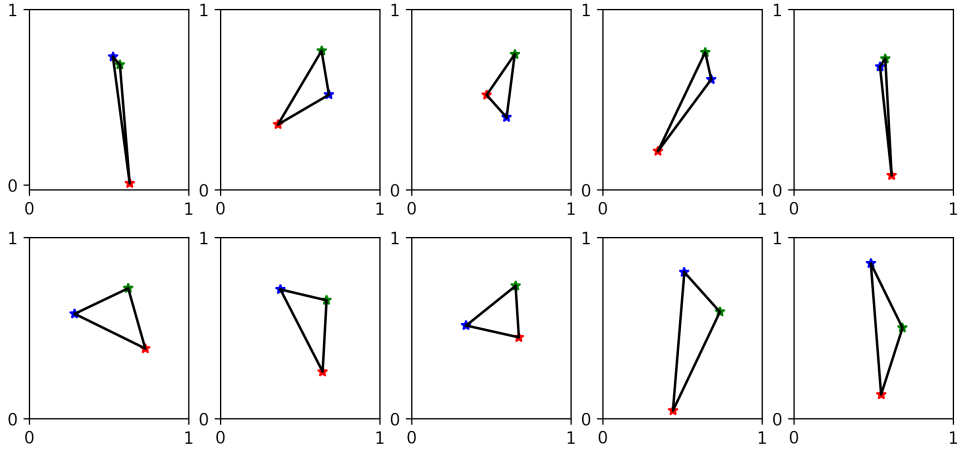

Fig. 5.2. Real data examples on $\mathcal{M} = St(3, 1)$.

5.1. Case 1: Numerical examples on $St(3, 1)$

These experiments concern the problem where observations are on the finite unit sphere. We consider this case for two reasons: i) First it is possible to visualize a path on the sphere

and ii) we validate our solution on the simplest example of Stiefel manifolds. Actually, this is a very common problem in many applications, e.g. virtual reality, autonomous driving, and robot navigation [4]. It is very known that geodesics exist and are unique for non antipodal points. Both the Riemannian exponential and its inverse are diffeomorphisms inside a ball of radius π. In all examples, we display the resulting path using the algorithm detailed in the paper and not a specific formulation for spherical data. We remind that the problem of regression with cubic splines can be efficiently solved in this case. However, our strategy is different: We show that the proposed method produces good estimators when the Stiefel manifold coincides with the sphere. Thus, and for visualization purposes, we consider the case $(n, p) = (3, 1)$ and show original data points (black) and the optimal α (red) with different values of N. The time instants are uniformly spaced in $[0, 1]$. See the three different examples in Fig. 5.3.

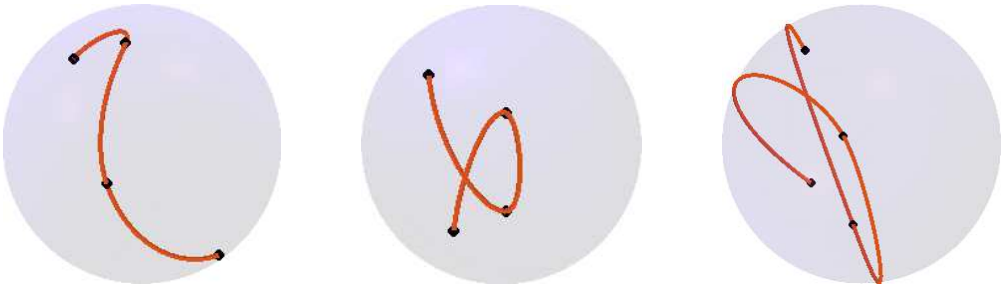

Fig. 5.3. Examples with different data points on $\mathcal{M} = St(3, 1)$.

5.2. Case 2: Numerical examples on $St(3, 2)$

These experiments concern the nonlinear regression problem where observations are elements of $\mathcal{M} = St(3, 2)$. They can be also considered as elements on the unit sphere, modulo rigid transformations, usually denoted Σ_n^p and called the Kendall space. They were largely studied for analyzing biological data [12]. We remind that our main objective is to show that the proposed method is successful in the case of $St(3, 2)$ and remains more general for other cases. Otherwise, geodesics, the exponential map, log map are detailed in [12]. We display the resulting path using the algorithm detailed in the paper and not a specific formulation for this manifold when equipped with a different structure. Our strategy is different: Demonstrate that the proposed method produces good estimators when the Stiefel manifold coincides with this manifold. For visualization purposes, we consider the case $(n, p) = (3, 2)$ and show the original data points and the optimal path α with different values of N. The time instants are uniformly spaced in $[0, 1]$. See Fig. 5.4 for an example of α interpolating $(X_0, X_1, X_2, X_3) \in St(3, 2)$ at $t \in \{0, 1/3, 2/3, 1\}$.

Following the same idea from the previous example in Fig. 5.4, we show another interpolating α using 5 points on $\mathcal{M} = St(3, 2)$ in Fig. 5.5. In the first example (X_1, X_2, X_3) are generated randomly in the ball $(X_0, 0.5\pi)$. In the second example (X_1, X_2, X_3, X_4) are generated randomly in the ball $(X_0, 0.25\pi)$. Considering the shape of the triangles and the coordinates (colored points) we can see that points in the first example are distant from each other compared to the second example but the changes along the path are smooth. Moreover, in the second example, X_2 and X_3 are very close and we observe the $\alpha(t)$ between them is quasi-constant. Same between X_3 and X_4, red and blue points are quasi-fixed while the green points are moving in the right direction smoothly. Another way to visualize the smoothness of α in the second example is to plot the norm of the first and second derivatives. We illustrate this

idea in Fig. 5.6 (top). In the same figure, we show the norm of the first and second derivatives of a piecewise geodesic path for comparison. We can easily check that the proposed solution is better.

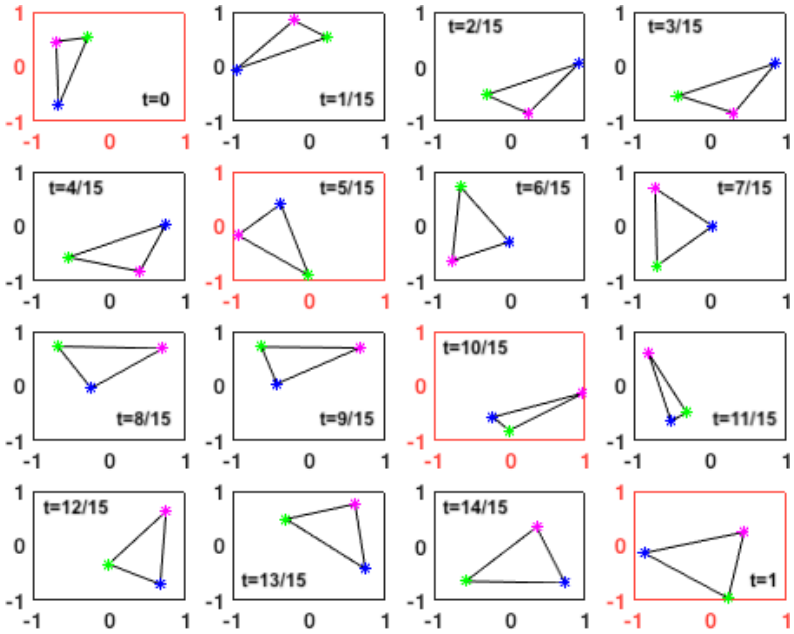

Fig. 5.4. Example of $\alpha(t)$, $t \in \{0, 1/15, \ldots, 1\}$ on $\mathcal{M} = St(3, 2)$. The original observations are given on the diagonal (red) at $t \in \{0, 1/3, 2/3, 1\}$. All $\alpha(t)$ are uniformly spaced in $[0, 1]$.

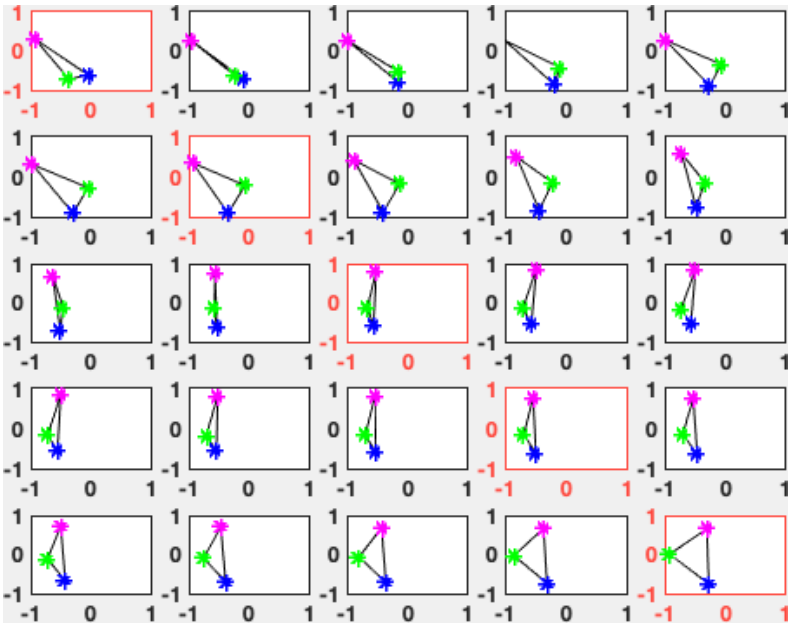

Fig. 5.5. Example of $\alpha(t)$, $t \in \{0, 1/25, \ldots, 1\}$ on $\mathcal{M} = St(3, 2)$. The original observations are given on the diagonal (red) and all $\alpha(t)$ are uniformly spaced in $[0, 1]$.

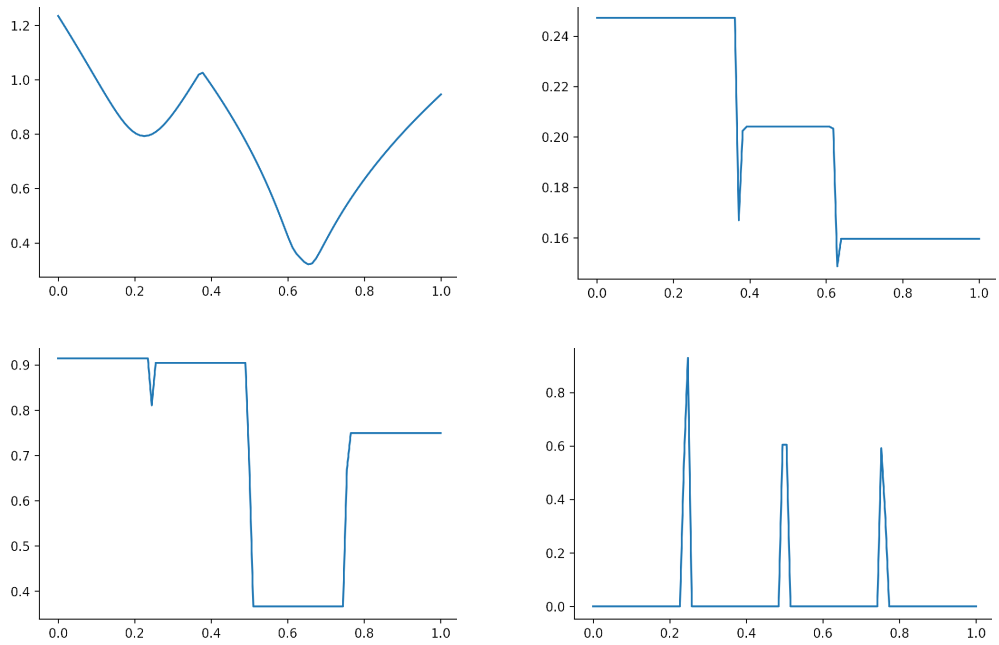

(a) (b)

Fig. 5.6. The norm of the first derivative (a) and the second derivative (b) of interpolating paths $\alpha(t)$, $t \in [0, 1]$ using the same example in Fig. 5.5. Top is the proposed solution and bottom is a piecewise geodesic path.

5.3. Case 3: Application on real data

A problem of great importance, and of current interest in the scientific community, is studying and exploiting electrocardiograms as a non-invasive methodology to detect heart diseases. While there are many successful works in the literature to study cardiological problems by means of static observations, there is still a need for mathematical models to study dynamic spatio-temporal changes. Thus, evolution between subjects or temporal observations for the same subject can help capture cross-sectional and functional variabilities [8]. In a medical context, such models can assist physicians in the interpretation of sequences. For example, they can be used to highlight changes during different temporal observations of the same subject. In this spirit, we present a new trajectory-based approach that can smoothly interpolate sequences observed from different subjects to study inter-subject variability (stages). We remind that our main goal is restricted to illustrating potential real applications without any medical interpretation of results.

We consider a real dataset of vectocardiograms (VCG) from children with ages varying between 2 and 19 where each observation $X_i = (x_i^1, x_i^2)$ belongs to $\mathcal{M} = St(3, 2)$ [30]. Each element describes the unitary vectors: x_i^1 as the direction to the apex and x_i^2 as the direction of motion. Fig. 5.7 represents each matrix observation $X_i = (x_i^1, x_i^2)$ by a points in $\mathcal{M} = St(3, 2)$. They are then interpolated by a path α in $\mathcal{M} = St(3, 2)$. The observations are displayed in red on the diagonal and all points $\alpha(t)$ are uniformly spaced in $[0, 1]$. To better visualize the dynamics along α, we show the norm of the first and second derivatives in Fig. 5.8 (top). We also show a piecewise geodesic path for comparison (bottom).

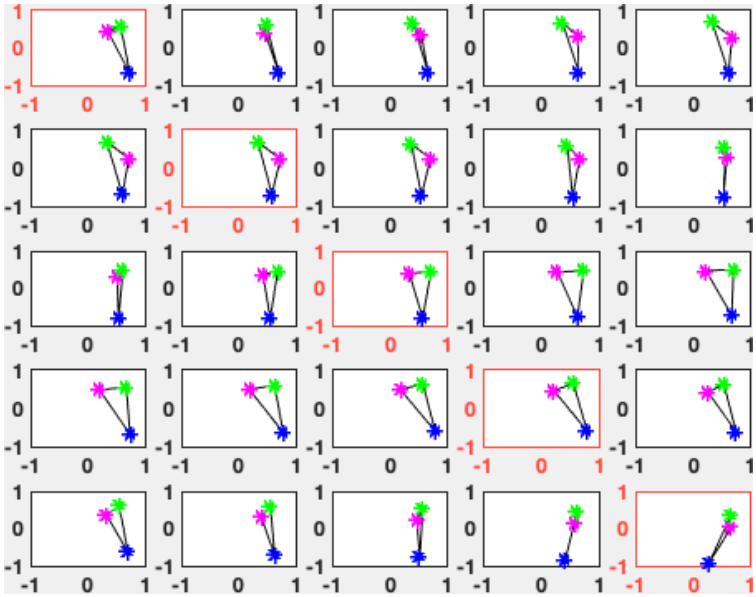

Fig. 5.7. Example of $\alpha(t)$, $t \in \{0, 1/25, \ldots, 1\}$ on $\mathcal{M} = St(3, 2)$. The original observations are given on the diagonal (red) and all $\alpha(t)$ are uniformly spaced in $[0, 1]$.

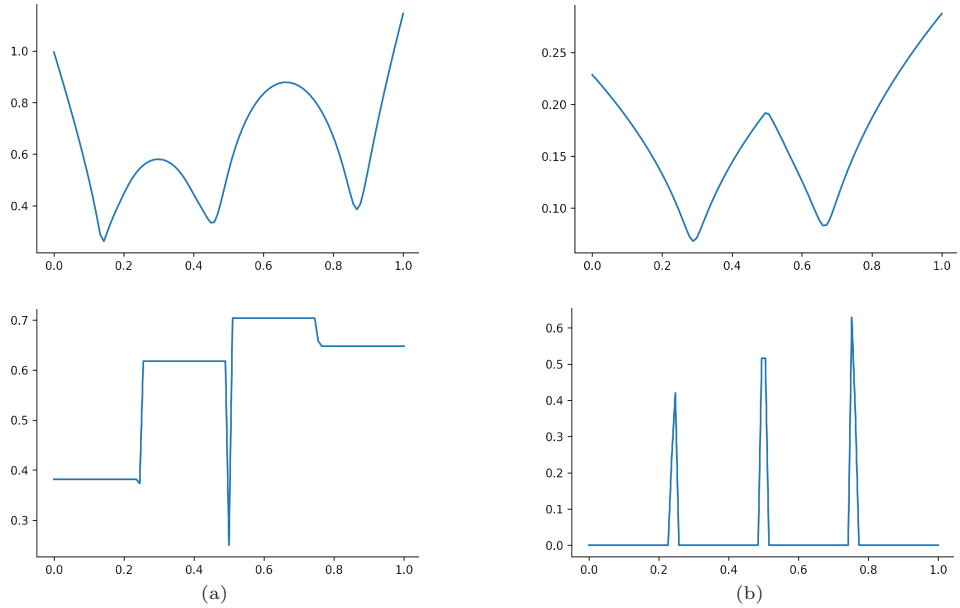

Fig. 5.8. The norm of the first derivative (a) and the second derivative (b) of interpolating paths $\alpha(t)$, $t \in [0, 1]$ using the same example in Fig. 5.7. Top is the proposed solution and bottom is piecewise geodesic path.

6. Conclusions

Given $X_0, \cdots, X_N$ a set of $(N + 1)$ distinct points on Stiefel and Grassmann manifolds $\mathcal{M}$ and $t_0 < t_1 < \cdots < t_N$ as an increasing sequence of time instants, we have introduced a new

framework for approximating a smooth curves that interpolate the given set of data points. We consider the Stiefel manifold as a quotient manifold of the orthogonal Lie group equipped with the inherited metric. With this geometric interpretation, we derive the explicit equations that generate control points of interpolating C^1 curves on Stiefel manifolds and C^2 splines on Grassmann manifolds due to the nice properties of this symmetric space. Our method is shown to posses a relatively low computational complexity and to be robust. The generalization of our method in general Homogeneous space is the major target of our future research.

Appendix A. C^2 Bézier Spline on $\mathbb{R}^n$

Let us consider the Euclidean case $\mathbb{R}^n$. Given a list of $(N+1)$ interpolation points $p_0, \cdots, p_N$ and for simplicity of the exposition we will assume that the time instants are $t_i = i$. In our case, throughout the construction of the piecewise-Bézier curve $\beta : [0, N] \longrightarrow \mathbb{R}^n$, we will only set $k \in \{2, 3\}$ such that the segment joining p_0 and p_1, as well as the segment joining p_{N-1} and p_N are Bézier curves of order two, while all the other segments are Bézier curves of order three. β_k are defined with a number of control points $\hat{b}_i$ represented as their coefficients in the Bernstein basis polynomials B_i^k. Explicitly, this means that

$$\beta_k\big(t; \widehat{b}_0, \cdots, \widehat{b}_k\big) = \sum_{i=0}^{k} \widehat{b}_i B_i^k(t).$$

Therefore, it is easily seen that the way we choose to define control points fully determines the curve β. In this case, we assume that there is two artificial control points $(\widehat{b}_i^-, \widehat{b}_i^+)$ on the left- and on the right-hand side of the interpolation point p_i, $i = 1, \ldots, N-1$. Consequently, β on $\mathbb{R}^n$ is given by

$$\beta(t) = \begin{cases} \beta_2\big(t; p_0, \widehat{b}_1^-, p_1\big), & \text{if} \quad t \in [0, 1], \\ \beta_3\big(t-(i-1); p_{i-1}, \widehat{b}_{i-1}^+, \widehat{b}_i^-, p_i\big), & \text{if} \quad t \in [i-1, i], \quad i = 2, \ldots, N-1, \\ \beta_2\big(t-(N-1); p_{N-1}, \widehat{b}_{N-1}^+, p_N\big), & \text{if} \quad t \in [N-1, N]. \end{cases}$$

It is easy to check that the interpolation conditions $\beta(t_i) = p_i$ holds and that $\beta|_{[t_i, t_{i+1}]}$ is smooth. Furthermore, to ensure that β is C^1, we shall make the following assumption:

$$\dot{\beta}_{k^i}\big(\widehat{b}_0^i, \cdots, \widehat{b}_{k^i}^i; t-i+1\big)\big|_{t=i} = \dot{\beta}_{k^{i+1}}\big(\widehat{b}_0^{i+1}, \cdots, \widehat{b}_{k^{i+1}}^{i+1}; t-i\big)\big|_{t=i}, \quad i = 0, \ldots, N-2. \tag{A.1}$$

This differentiability condition allows us to express $\widehat{b}_i^+$ in terms of $\widehat{b}_i^-$ as

$$\widehat{b}_1^+ = \frac{5}{3} p_1 - \frac{2}{3} \widehat{b}_1^-, \tag{A.2}$$

$$\widehat{b}_i^+ = 2p_i - \widehat{b}_i^-, \quad i = 2, \ldots, N-2, \tag{A.3}$$

$$\widehat{b}_{N-1}^+ = \frac{5}{2} p_{N-1} - \frac{3}{2} \widehat{b}_{N-1}^-. \tag{A.4}$$

Hence, the task now is reduced to search only control points $\widehat{b}_i^-$, $i = 1, \ldots, N-1$, that generate the C^1 Bézier spline β in $\mathbb{R}^n$. Replacing the new optimization variables in problem (1.1) gives (3.1), which is merely the problem of minimization of the mean square acceleration of the Bézier

curve β in the Euclidean space $\mathbb{R}^n$

$$\begin{aligned}\min_{\widehat{b}_1^-,\cdots,\widehat{b}_{N-1}^-} E\big(\widehat{b}_1^-,\cdots,\widehat{b}_{N-1}^-\big) := \min_{\widehat{b}_1^-,\cdots,\widehat{b}_{N-1}^-} &\int_0^1 \big\|\ddot{\beta}_2^0\big(t;p_0,\widehat{b}_1^-,p_1\big)\big\|^2 \\ &+ \sum_{i=1}^{N-2}\int_0^1 \big\|\ddot{\beta}_3^i\big(t;p_i,\widehat{b}_i^-,\widehat{b}_{i+1}^-,p_{i+1}\big)\big\|^2 \\ &+ \int_0^1 \big\|\ddot{\beta_2^{N-1}}\big(t;p_{N-1},\widehat{b}_{N-1}^-,p_N\big)\big\|^2. \end{aligned} \tag{A.5}$$

Minimizing the functional E requires the computation of its gradient and then the search of its critical points. As the energy is based on polynomials, it is possible to compute the analytical expression of its gradient. We first compute the acceleration on respective intervals and then evaluate the integral of each term of Eq. (A.5). For brevity, we skip the details and we give just the final formulation of Eq. (A.5) which allows us to determine the optimal solution. After simplification, we have

$$\begin{aligned}\min_{\widehat{b}_1^-,\cdots,\widehat{b}_{N-1}^-} E\big(\widehat{b}_1^-,\cdots,\widehat{b}_{N-1}^-\big) := 4\Big(&-4p_0^T\widehat{b}_1^- + 4\widehat{b}_1^{-T}\widehat{b}_1^- - 4p_1^T\widehat{b}_1^-\Big) \\ &+ \sum_{i=1}^{N-2} 36\Big(-p_i^T\widehat{b}_i^+ + \widehat{b}_i^{+T}\widehat{b}_i^+ - \widehat{b}_i^{+T}\widehat{b}_{i+1}^- + \widehat{b}_{i+1}^{-T}\widehat{b}_{i+1}^- - \widehat{b}_{i+1}^{-T}p_{i+1}\Big) \\ &+ 4\Big(-4p_{N-1}^T\widehat{b}_{N-1}^+ + 4\widehat{b}_{N-1}^{+T}\widehat{b}_{N-1}^+ - 4p_N^T\widehat{b}_{N-1}^+\Big) + K, \end{aligned} \tag{A.6}$$

where K denotes a constant term involving all p_i. Next we replace $\widehat{b}_i^+$'s by $\widehat{b}_i^-$'s using Eqs. (A.2)-(A.4). Then the optimal solution is given by

$$\begin{aligned}
&\frac{\partial E}{\partial \widehat{b}_1^-} = 4\big(8\widehat{b}_1^- - 4p_0 - 4p_1\big) + 36\left(-\frac{14}{9}p_1 + \frac{8}{9}\widehat{b}_1^- + \frac{6}{9}\widehat{b}_2^-\right) = 0,\\
&\frac{\partial E}{\partial \widehat{b}_2^-} = 36\left(-\frac{5}{3}p_1 + \frac{2}{3}\widehat{b}_1^- + 2\widehat{b}_2^- - p_2\right) + 36\big(-3p_2 + 2\widehat{b}_2^- + \widehat{b}_3^-\big) = 0,\\
&\frac{\partial E}{\partial \widehat{b}_j^-} = 36\big(-3p_j + 2\widehat{b}_j^- + \widehat{b}_{j+1}^-\big)\\
&\qquad + 36\big(-2p_{j-1} + \widehat{b}_{j-1}^- + 2\widehat{b}_j^- - p_j\big) = 0, \quad j = 2,\ldots,N-2,\\
&\frac{\partial E}{\partial \widehat{b}_{N-1}^-} = 36\big(-2p_{n-2} + \widehat{b}_{N-2}^- + 2\widehat{b}_{N-1}^- - p_{N-1}\big) + 4\big(-24p_{N-1} + 18\widehat{b}_{N-1}^- + 6p_N\big) = 0.
\end{aligned} \tag{A.7}$$

The optimal solution $Y = [\widehat{b}_1^-,\cdots,\widehat{b}_{N-1}^-]^T \in \mathbb{R}^{(N-1)\times m}$ of that problem is the unique solution of a tridiagonal linear system

$$Y = A^{-1}CP = DP \quad \text{with} \quad \sum_{j=0}^{j=N+1} d_{ij} = 1, \tag{A.8}$$

where A is a tridiagonal sparse square matrix of size $(N-1)\times(N-1)$ with a dominant diagonal, C a matrix of size $(N-1)\times(N+1)$ and P the matrix of p_i's of size $(N+1)\times m$ given by

$$A_{(1,1:2)} = [16\ 6], \tag{A.9}$$

$$A_{(2,1:3)} = [6\ 36\ 9], \tag{A.10}$$
$$A_{(i,i-1:i+1)} = [9\ 36\ 9], \tag{A.11}$$
$$A_{(n-1,n-2:n-1)} = [9\ 36], \tag{A.12}$$
$$C_{(1,1:2)} = [16\ 6], \tag{A.13}$$
$$C_{(2,2:3)} = [6\ 36\ 9], \tag{A.14}$$
$$C_{(i,i:i+1)} = [9\ 36\ 9], \quad i = 3, \dots, n-2. \tag{A.15}$$
$$C_{(n-1,n-1:n+1)} = [9\ 36]. \tag{A.16}$$

We may now write the C^2 differentiability condition. It is obvious that with this C^2 condition the position of the control points $\widehat{b}_i^-$ and $\widehat{b}_i^+$ that generate the curve β will be modified. Therefore, it is more convenient to use another notation. Let us denote by b_i^- and b_i^+ the new control points on the left- and on the right-hand side of the interpolation point p_i, $i = 1, \dots, N-1$. Computing the acceleration of β on respective intervals and taking into account that β is C^1, we shall replace b_1^+ by (A.2), b_i^+ by (A.3), and b_{N-1}^+ by (A.4). We deduce that

$$b_2^- = \frac{1}{3}p_0 - \frac{1}{2}b_1^- + \frac{8}{3}p_1, \tag{A.17}$$
$$b_{i+1}^- = b_{i-1}^+ + 4p_i - 4b_i^-, \quad i = 2, \dots, N-2, \tag{A.18}$$
$$p_N = 2p_{N-1} + 2b_{N-1}^+ - 6b_{N-1}^- + 3b_{N-2}^+. \tag{A.19}$$

We see at once that points that will be modified by the additional C^2 condition are $\widehat{b}_i^-$ and hence, $\widehat{b}_i^+$, $i = 2, \dots, N-1$. The point $\widehat{b}_1^-$ remains invariant and consequently it will be the case for $\widehat{b}_1^+$. According to the C^1 differentiability condition ensured at the first step, one can take $b_1^- = \widehat{b}_1^-$, with $\widehat{b}_1^-$ is the first row of the matrix Y obtained as a solution of the optimization problem (3.1). However, the endpoint p_n is affected as we can deduce from Eq. (A.19). Nevertheless, it follows that giving the control point b_1^- allows us to find all the other control points including b_2^- with Eq. (A.17) and hence, b_2^+ with (A.3), then b_{i+1}^-, $i = 2, \dots, N-2$ with (A.18) and therefore b_i^+, $i = 3, \dots, N-2$ with (A.3) and b_{N-1}^+ with (A.4).

Appendix B. Proof of Theorem 4.2

We now prove Theorem 4.2. The proof is based on the following two results given in [33].

Lemma B.1. *Let $X_1 \in \mathcal{M}$.*

1. $(d\varphi_{X_1})^{-1}_{X_2} = (d\varphi_{X_1})_{\varphi_{X_1}(X_2)}$ *for all* $X_2 \in \mathcal{M}$.
2. $(d\varphi_{X_1})_{\mathrm{Exp}_{X_1}(H)} \circ (d\mathrm{Exp}_{X_1})_H = -(d\mathrm{Exp}_{X_1})_{-H}$ *for all* $H \in T_{X_1}\mathcal{M}$.

Theorem B.1. *Let $t \longrightarrow \alpha_j(t, V_0, \cdots, V_j)$ be the Bézier curve of order j on $\mathcal{M}$ with a number of control points V_j, $i = 0, \dots, j$. Then $\alpha_j(t; V_0, \cdots, V_j)$ satisfies*

1. $\left.\dfrac{D}{dt}\right|_{t=0} \dot{\alpha}_j(t; V_0, \cdots, V_j) = j(j-1)\Omega_0$, *where*

$$\Omega_0 := \begin{cases} \dot{\gamma}(0, V_1, V_2), & \text{if} \quad V_0 = V_1, \\ \big(d\mathrm{Exp}_{V_0}\big)^{-1}_{\dot{\gamma}(0,V_0,V_1)}\big(\dot{\gamma}(0, V_1, V_2) - \dot{\gamma}(1, V_0, V_1)\big), & \text{if} \quad V_0 \neq V_1. \end{cases}$$

2. $\left.\dfrac{D}{dt}\right|_{t=1} \dot{\alpha}_j(t; V_0, \cdots, V_j) = j(j-1)\Omega_j$, *where*

$$\Omega_j := \begin{cases} -\dot{\alpha}\big(0, V_{j-2}, V_{j-1}\big), & \text{if} \quad V_{j-1} = V_j, \\ \big(d\mathrm{Exp}_{V_j}\big)^{-1}_{-\dot{\alpha}(1,V_{j-1},V_j)}\big(\dot{\alpha}(0, V_{j-1}, V_j) - \dot{\alpha}(1, V_{j-2}, V_{j-1})\big), & \text{if} \quad V_{j-1} \neq V_j. \end{cases}$$

We will exploit a modified form of the Theorem B.1 to obtain the proof of Theorem 4.1.

Proof of Theorem 4.1. The Bézier curve α is C^2 on $\mathcal{M}$ if and only if it satisfies the C^2 differentiability condition at joint points $\tilde{X}_i$, $i = 1, \ldots, n-1$. At the point $\tilde{X}_1$, this means

$$\left.\frac{D}{dt}\right|_{t=1} \dot{\alpha}_2\big(t; \tilde{X}_0, Y_1^-, \tilde{X}_1\big) = \left.\frac{D}{dt}\right|_{t=0} \dot{\alpha}_3\big(t; \tilde{X}_1, Y_1^+, Y_2^-, \tilde{X}_2\big). \tag{B.1}$$

Applying Theorem B.1 yields: α is C^2 on $\tilde{X}_1$ if and only if $\Omega_2 - 3\Omega_0 = 0$ with

$$\begin{aligned} \Omega_2 - 3\Omega_0 = {} & \big(d\mathrm{Exp}_{\tilde{X}_1}\big)^{-1}_{-\dot{\gamma}(1,Y_1^-,\tilde{1})}\Big(\dot{\gamma}\big(0, Y_1^-, \tilde{X}_1\big) - \dot{\gamma}\big(1, \tilde{X}_0, Y_1^-\big)\Big) \\ & - 3\big(d\mathrm{Exp}_{\tilde{X}_1}\big)^{-1}_{\dot{\gamma}(0,\tilde{X}_1,Y_1^+)}\Big(\dot{\gamma}\big(0, Y_1^+, Y_2^-\big) - \dot{\gamma}\big(1, \tilde{X}_1, Y_1^+\big)\Big). \end{aligned} \tag{B.2}$$

Since β_1 is a C^1 Bézier curve on $T_{X_1}\mathcal{M}$, we have that $\dot{\gamma}(1, Y_1^-, \tilde{X}_1) = \dot{\gamma}(0, \tilde{Y}_1, Y_1^+)$. By Lemma B.1, we have

$$\begin{aligned} & \big(d\mathrm{Exp}_{\tilde{X}_1}\big)^{-1}_{\dot{\gamma}(0,\tilde{X}_1,Y_1^+)}\Big(\dot{\gamma}\big(0, Y_1^+, Y_2^-\big) - \dot{\gamma}\big(1, \tilde{X}_1, Y_1^+\big)\Big) \\ = {} & -\big(d\mathrm{Exp}_{\tilde{X}_1}\big)^{-1}_{-\dot{\gamma}(0,\tilde{X}_1,Y_1^+)}\Big((d\varphi_{\tilde{X}_1})_{Y_1^+}\big(\dot{\gamma}\big(0, Y_1^+, Y_2^-\big) - \dot{\alpha}\big(1, \tilde{X}_1, Y_1^+\big)\big)\Big). \end{aligned}$$

It follows that

$$\begin{aligned} \Omega_2 - 3\Omega_0 = {} & \big(d\mathrm{Exp}_{\tilde{X}_1}\big)^{-1}_{-\dot{\gamma}(0,\tilde{X}_1,Y_1^+)}\Big(\dot{\gamma}\big(0, Y_1^-, \tilde{X}_1\big) - \dot{\gamma}\big(1, \tilde{X}_0, Y_1^-\big)\Big) \\ & + 3\big(d\mathrm{Exp}_{\tilde{X}_1}\big)^{-1}_{-\dot{\gamma}(0,\tilde{X}_1,Y_1^+)}\Big((d\varphi_{\tilde{X}_1})_{Y_1^+}\big(\dot{\gamma}\big(0, Y_1^+, Y_2^-\big) - \dot{\gamma}\big(1, \tilde{X}_1, \chi_1^+\big)\big)\Big) \\ = {} & \big(d\mathrm{Exp}_{\tilde{X}_1}\big)^{-1}_{-\dot{\gamma}(0,\tilde{X}_1,Y_1^+)}\Big[3(d\varphi_{\tilde{X}_1})_{Y_1^+}\big(\dot{\gamma}\big(0, Y_1^+, Y_2^-\big)\big) - 3(d\varphi_{\tilde{X}_1})_{Y_1^+}\big(\dot{\gamma}\big(1, \tilde{X}_1, Y_1^+\big)\big) \\ & \qquad + \dot{\gamma}\big(0, Y_1^-, \tilde{X}_1\big) - \dot{\gamma}\big(1, \tilde{X}_0, Y_1^-\big)\Big]. \end{aligned}$$

Hence, $\Omega_2 - 3\Omega_0 = 0$ if and only if

$$\begin{aligned} & 3(d\varphi_{\tilde{X}_1})_{Y_1^+}\Big(\dot{\gamma}\big(0, X_1^+, Y_2^-\big)\Big) - 3(d\varphi_{\tilde{X}_1})_{Y_1^+}\Big(\dot{\gamma}\big(1, \tilde{X}_1, Y_1^+\big)\Big) \\ & \quad + \dot{\alpha}\big(0, Y_1^-, \tilde{X}_1\big) - \dot{\gamma}\big(1, \tilde{X}_0, Y_1^-\big) = 0. \end{aligned} \tag{B.3}$$

Nevertheless

$$\varphi_{\tilde{X}_1}\Big(\gamma\big(t, \tilde{X}_1, Y_1^+\big)\Big) = \alpha\big(1-t, Y_1^-, \tilde{X}_1\big), \quad \forall t \in [0,1].$$

Differentiate this identity with respect to t, we obtain

$$(d\varphi_{\tilde{X}_1})_{Y_1^+}\Big(\dot{\gamma}\big(1, \tilde{X}_1, Y_1^+\big)\Big) = -\dot{\gamma}\big(0, Y_1^-, \tilde{X}_1\big).$$

Accordingly, Eq. (B.3) becomes

$$3(d\varphi_{\tilde{X}_1})_{Y_1^+}\Big(\dot{\gamma}\big(0, Y_1^+, Y_2^-\big)\Big) = \dot{\gamma}\big(1, \tilde{X}_0, Y_1^-\big) - 4\dot{\gamma}\big(0, Y_1^-, \tilde{X}_1\big). \tag{B.4}$$

Now, Lemma B.1 shows that

$$\begin{aligned}(d\varphi_{\tilde{X}_1})_{Y_1^+}\Big(\dot\gamma\big(0,Y_1^+,Y_2^-\big)\Big) &= (d\varphi_{\tilde{X}_1})_{\varphi_{\tilde{X}_1}\left(Y_1^-\right)}\Big(\dot\gamma\big(0,Y_1^+,Y_2^-\big)\Big)\\ &= (d\varphi_{\tilde{X}_1})^{-1}_{Y_1^-}\Big(\dot\gamma\big(0,Y_1^+,Y_2^-\big)\Big).\end{aligned}$$

It follows that

$$(d\varphi_{\tilde{X}_1})^{-1}_{Y_1^-}\Big(\dot\gamma\big(0,Y_1^+,Y_2^-\big)\Big) = \frac{1}{3}\Big(\dot\gamma\big(1,\tilde{X}_0,Y_1^-\big) - 4\dot\gamma\big(0,Y_1^-,\tilde{X}_1\big)\Big).$$

Consequently, with the exponential map at the point χ_1^+, we get

$$Y_2^- = \mathrm{Exp}_{Y_1^+}\left(\frac{1}{3}\big((d\varphi_{\tilde{X}_1})_{Y_1^-}\big(\dot\gamma(1,\tilde{X}_0,Y_1^-)\big) - 4\dot\alpha\big(0,Y_1^-,\tilde{X}_1\big)\big)\right). \tag{B.5}$$

The proof of Part (iii) follows in much the same way as Part (ii). □

Acknowledgements. This work was partially funded by the CNRS PRIME.

References

[1] P.A. Absil, R. Mahony, and R. Sepulchre, *Optimization Algorithms on Matrix Manifolds*, Princeton University Press, 2008.

[2] A. Arnould, P.Y. Gousenbourger, C. Samir, P.A. Absil, and M. Canis, Fitting smooth paths on Riemannian manifolds: Endometrial surface reconstruction and preoperative MRI-based navigation, in: *Geometric Science of Information*, Springer, **9389** (2015), 491–498.

[3] E. Batzies, K. Hüper, L. Machado, and F. Silva Leite, Geometric mean and geodesic regression on Grassmannians, *Linear Algebra Appl.*, **466** (2015), 83–101.

[4] T. Bendory, S. Dekel, and A. Feuer, Super-resolution on the sphere using convex optimization, *IEEE Trans. Signal Process.*, **63**:9 (2015), 2253–2262.

[5] D. Bryner, Endpoint geodesics on the Stiefel manifold embedded in Euclidean space, *SIAM J. Matrix Anal. Appl.*, **38** (2017), 1139–1159.

[6] R. Chakraborty and B.C. Vemuri, Statistics on the compact Stiefel manifold: Theory and applications, *Ann. Statist.*, **47**:1 (2017), 415–438.

[7] A. Cherian and J. Wang, Generalized one-class learning using pairs of complementary classifiers, *IEEE Trans. Pattern Anal. Mach. Intell.*, **43**:2 (2021), 420–433.

[8] A. Cholaquidis, R. Fraiman, F. Gamboa, and L. Moreno, Weighted lens depth: Some applications to supervised classification, *Canad. J. Statist.*, **51**:2 (2023), 652–673.

[9] P. Clément, B. Guillaume, and C. Vincent, Improved time-series clustering with UMAP dimension reduction method, in: *25th International Conference on Pattern Recognition*, (2021), 5658–5665.

[10] P. Crouch, G. Kun, and F. Silva Leite, The de Casteljau algorithm on Lie groups and spheres, *J. Dyn. Control Syst.*, **5** (1999), 397–429.

[11] P. De Casteljau, *Outillages Méthodes de Calcul*, Institute National de la Propriété Industrielle, 1959.

[12] I.L. Dryden and K.V. Mardia, *Statistical Shape Analysis: With Applications in R*, John Wiley and Sons, 2016.

[13] N. Dyn, Linear and nonlinear subdivision schemes in geometric modeling, in: *Foundations of Computational Mathematics*, (2009), 68–92.

[14] A. Edelman, T.A. Arias, and S.T. Smith, The geometry of algorithms with orthogonality constraints, *SIAM J. Matrix Anal. Appl.*, **20**:2 (1998), 303–353.

[15] B. Geir, M. Klas, and V. Olivier, Numerical algorithm for C^2-splines on symmetric spaces, *SIAM J. Numer. Anal.*, **56**:4 (2018), 2623–2647.

[16] P.-Y. Gousenbourger, C. Samir, and P.A. Absil, Piecewise-Bézier C^1 Interpolation on Riemannian manifolds with application to 2D shape morphing, *IEEE ICP*, (2014), 4086–4091.

[17] J. Hinkle, P.T. Fletcher, and S. Joshi, Intrinsic polynomials for regression on Riemannian manifolds, *J. Math. Imaging Vision*, **50** (2014), 32–52.

[18] Y. Hong, R. Kwitt, N. Singh, B. Davis, N. Vasconcelos, and M. Niethammer, Geodesic regression on the Grassmannian, in: *European Conference on Computer Vision ECCV*, (2014), 632–646.

[19] K. Hüper, U. Helmke, and S. Herzberg, On the computation of means on Grassmann manifolds, in: *Proceedings of the 19th International Symposium on Mathematical Theory of Networks and Systems*, (2010), 2439–2441.

[20] K. Hüper and F. Silva Leite, On the geometry of rolling and interpolation curves on S^n, $SO(n)$, and Grassmann manifolds, *J. Dyn. Control Syst.*, **13**:4 (2007), 467–502.

[21] P.E. Jupp and J.T. Kent, Fitting smooth paths to speherical data, *J. Appl. Stat.*, **36**:1 (1987), 34–46.

[22] K.R. Kim, I.L. Dryden, and H. Le, Smoothing splines on Riemannian manifolds with applications to 3D shape space, *J. R. Stat. Soc. Ser. B. Stat. Methodol.*, **83**:1 (2020), 108–132.

[23] K.A. Krakowski, L. Machado, F. Silva Leite, and J. Batista, A modified Casteljau algorithm to solve interpolation problems on Stiefel manifolds, *J. Comput. Appl. Math.*, **311** (2017), 84–99.

[24] G. Kyle, S. Anuj, L. Xiuwen, and V.D. Paul, Efficient algorithms for inferences on Grassmann manifolds, in: *Proceedings of 12th IEEE Workshop on Statistical Signal Processing*, (2003), 315–318.

[25] D.S. Lee, A.K. Sahib, K.L. Narr, E. Nunez and S. Joshi, Global diffeomorphic phase alignment of time-series from resting-state fMRI data, *Med. Image Comput. Comput. Assist. Interv.*, **12267** (2020), 518–527.

[26] L. Lin, B. St Thomas, H. Zhu, and D.B. Dunson, Extrinsic local regression on manifold-valued data, *J. Amer. Statist. Assoc.*, **112**:519 (2017), 1261–1273.

[27] G. Mustafa and R. Hameed, Families of non-linear subdivision schemes for scattered data fitting and their non-tensor product extensions, *Appl. Math. Comput.*, **359** (2019), 214–240.

[28] M. Niethmmer, Y. Huang, and F.-X. Vialard, Geodesic regression for image time-series, in: *International Conference on Medical Image Computing and Computer-Assisted Intervention*, **6892** (2011), 655–662.

[29] Y. Nishimori and S. Akaho, Learning algorithms utilizing quasi-geodesic flows on the Stiefel manifold, *Neurocomputing*, **67** (2005), 106–135.

[30] S. Pal, S. Sengupta, R. Mitra, and A. Banerjee, A Bayesian approach for analyzing data on the Stiefel manifold, *arXiv:1907.04303*, 2019.

[31] A. Petersen and H.G. Müller, Fréchet regression for random objects with Euclidean predictors, *Ann. Statist.*, **47**:2 (2019), 691–719.

[32] T. Popiel and L. Noakes, C^2 spherical Bézier splines, *Comput. Aided Geom. Des.*, **23** (2006), 261–275.

[33] T. Popiel and L. Noakes, Bézier curves and C^2 interpolation in Riemannian manifolds, *J. Approx. Theory*, **148**:2 (2007), 111–127.

[34] Q. Rentmeesters, A gradient method for geodesic data fitting on some symmetric Riemannian manifolds, in: *Proceedings of the IEEE Conference on Decision and Control*, (2011), 7141–7146.

[35] Q. Rentmeesters, P.A Absil, P. Van Dooren, K. Gallivan, and A. Srivastava, An efficient particle filtering technique on the Grassmann manifold, in: *2010 IEEE International Conference on Acoustics, Speech and Signal Processing*, (2010), 3838–3841.

[36] C. Samir, P.-A. Absil, A. Srivastava, and E. Klassen, A gradient-descent method for curve fitting on Riemannian manifolds, *Found. Comput. Math.*, **12** (2012), 49–73.

[37] T. Shingel, Interpolation in special orthogonal groups, *IMA J. Numer. Anal.*, **29**:3 (2009), 731–745.

[38] F. Silva Leite and L. Machado, Fitting smooth paths on Riemannian manifolds, *Int. J. Appl.*

Math. Stat., **06**:4 (2006), 25–53.

[39] A. Srivastava and E. Klassen, *Functional and Shape Data Analysis*, Springer, 2016.

[40] G. Sundaramoorthi, A. Mennucci, S. Soatto, and A.J. Yezzi, A new geometric metric in the space of curves, and applications to tracking deforming objects by prediction and filtering, *SIAM J. Imaging Sci.*, **4**:1 (2011), 109–145.

[41] J. Wallner, E. Nava Yazdani, and P. Grohs, Smoothness properties of Lie group subdivision schemes, *Multiscale Model. Simul.*, **6**:2 (2007), 493–505.

[42] R. Zhang, L. Xuelong, H. Zhang, and Z. Jiao, Geodesic multi-class SVM with Stiefel manifold embedding, *IEEE Trans. Pattern Anal. Mach. Intell.*, 2021. doi: 10.1109/TPAMI.2021.3069498

[43] R. Zimmermann, A matrix-algebraic algorithm for the Riemannian logarithm on the Stiefel manifold under the canonical metric, *SIAM J. Matrix Anal. Appl.*, **38**:2 (2017), 322–342.